# Examination of the phenomenological scaling functions for critical scattering

Craig A. Tracy*
*Institute for Fundamental Studies, Department of Physics and Astronomy, University of Rochester, Rochester, New York 14627*

Barry M. McCoy†‡
*Institute for Theoretical Physics, State University of New York at Stony Brook, Stony Brook, New York 11794*
(Received 6 February 1975)

In the scaling limit $k\to 0$, $\xi\to\infty$ such that $y=k\xi$ is fixed, the $k$-dependent susceptibility $\chi(\vec{k},T)$ can, according to the scaling hypotheses of Kadanoff and Fisher, be written as $\chi(\vec{k},T) = \xi^{\gamma/\nu}X_{\pm}(y)+o(\xi^{\gamma/\nu})$. We exactly compute the scale functions $X_{\pm}(y)$ for the two-dimensional Ising model in zero magnetic field. We then compare the various phenomenological scale functions (Ornstein-Zernike pole approximate, Fisher approximate, Fisher-Burford approximate, Tarko-Fisher approximates, etc.) with the exact $X_{\pm}(y)$ for the two-dimensional Ising model. This comparison provides insight into those regions of $y = k\xi$ where these phenomenological scale functions are applicable. Such insight is important since the region of experimentally accessible $y$ is rather limited. We then use these results to examine the method of data analysis used in critical scattering experiments. We conclude that no experiment to date unambiguously and directly establishes that the critical exponent $\eta$ is greater than zero.

## I. INTRODUCTION

In the past decade a great amount of study has been given to $\chi(\vec{k}, T)$ (the $\vec{k}$-dependent susceptibility) in the scaling region where

$$T\to T_c, \quad k\to 0, \tag{1.1}$$

such that if $\xi(T)$ is the correlation length

$$y=k\xi(T) \tag{1.2}$$

is fixed. For a magnetic system $\chi(\vec{k}, T)$ is the Fourier transform of the spin-spin correlation function [and for a fluid $\chi(\vec{k}, T)$ is the Fourier transform of the density-density correlation function]. As $T\to T_c$ the correlation length $\xi(T)$ and the thermodynamic susceptibility $\chi(0, T)$ diverge and are usually parameterized as

$$\xi\sim\xi_0^{\pm}|1-T/T_c|^{-\nu} \tag{1.3}$$

and

$$\chi(0,T)\sim C_{0\pm}|1-T/T_c|^{-\gamma} \tag{1.4}$$

[where + (−) denotes that $T\to T_c$ from above (below)]. In the limit (1.1) and (1.2) Kadanoff[1] and Fisher[2,3] assume that $\chi(\vec{k}, T)$, which is a function of the two variables $\vec{k}$ and $T$, reduces to essentially a function of one variable

$$\chi(\vec{k}, T)=\xi^{\gamma/\nu}X_{\pm}(y)+o(\xi^{\gamma/\nu}) . \tag{1.5}$$

The functions $X_{\pm}(y)$ are referred to as scaling functions.

In general $X_{\pm}(y)$ are functions which depend on the system under consideration. However, for physically realistic systems no exact calculation of $X_{\pm}(y)$ has ever been carried out. Therefore, studies of $X_{\pm}(y)$ have been of an approximate nature, and over the years a large number[2,4–10] of approximates to $X_{\pm}(y)$ have been proposed. The most famous of these phenomenological approximates is that of Ornstein and Zernike,[4]

$$X_{\mathrm{OZ}}(y)=x_0(1+y^2)^{-1} , \tag{1.6}$$

while some of the more recent approximates are those of Fisher,[2]

$$X_{\mathrm{F}}(y)=A(1+y^2)^{-1+\eta/2} , \tag{1.7}$$

and of Fisher and Burford,[5]

$$X_{\mathrm{FB}}(y)=A\frac{(1+\phi_c^2y^2)^{\eta/2}}{1+y^2} . \tag{1.8}$$

Each proposed approximate scaling function has certain virtues in that each incorporates some general feature which $X_{\pm}(y)$ is expected to possess. However, without some exact $X_{\pm}(y)$ it is impossible to fully assess either the range of $y$ over which the approximates are expected to be useful or the quantitative accuracy of the approximates. It is the primary purpose of this paper to make such a detailed study of these phenomenological approximates by comparing them with the Fourier transform of the exact spin-spin correlation function of the two-dimensional Ising model in the scaling limit.[11–13]

In Sec. II we examine the analytic structure of the scale functions $X_{\pm}(y)$ for the two-dimensional Ising model in zero magnetic field. To keep the mathematical derivations to a minimum, we put all computations into a series of appendixes so that in Sec. II only the barest facts concerning $X_{\pm}(y)$ are presented. However even this may not be of

interest to the general reader who is most interested in our conclusions concerning critical-scattering phenomenology and experiments. If this is the case we recommend that the reader only look at Figs. 1 and 2, and begin reading at Sec. III, and only when necessary (or interested) go back and read the relevant results of Sec. II.

In Sec. III we give a detailed comparison of the various scattering approximates [i.e., Ornstein-Zernike pole approximate (1.6), Fisher approximate (1.7), Fisher-Burford approximate (1.8), Tarko-Fisher approximates,[8] etc.] with the exact results of the two-dimensional Ising model. This comparison will provide insight into the regions of $y$ ($=k\xi$) where these formulas are applicable (for example, how large does $y$ have to be before the Fisher approximate is good to 5%?). Such insight is important since the region of experimentally accessible $y$ is rather limited at present (the largest values[14–24] of $y$ range up to no more than 65, but perhaps 20 to 30 is more typical). Thus one does not want to use a phenomenological formula for some scale function that is not expected to be valid in the range of $y$ in which the experiment is conducted. Table V summarizes these results.

In Sec. IV we use our six-place values of the scale function $X_{\pm}(y)$ as "data" over varying ranges of $y$ and try by using various phenomenological scaling functions (Fisher approximate, Fisher-Burford approximate, etc.) as fitting functions in a least-squares program to extract the critical exponent $\eta$. The exponent $\eta$ is defined[2] by the large-$y$ behavior of $X_{\pm}(y)$,

$$X_{\pm}(y) \sim C_1 y^{-2+\eta}, \quad y \to \infty \tag{1.9}$$

and the scaling theories of Kadanoff[1] and Fisher[2,3] predict that $\eta$ is related to $\gamma$ and $\nu$ [see (1.3) and (1.4)] by the relation

$$(2-\eta)\nu = \gamma . \tag{1.10}$$

The results of our least-squares "experiment" are summarized in Table VI. These results will then lead us to conclude that *no experiments[14–23] to date clearly and unambiguously establish that* $\eta > 0$. We then discuss what we feel would be an unambiguous determination of $\eta$. We recommend that this procedure (which depends upon use of the Fisher-Langer[25] approximate) be used in the future rather than the methods that have previously been used.[26]

## II. DISPERSION REPRESENTATION OF $X_{\pm}(y)$

For the two-dimensional Ising model in zero magnetic field we find that the scale functions $X_{\pm}(y)$ of (1.5) [see Appendix A for a precise definition of $\xi$ and $y$ in terms of the interaction energies $E_1$ and $E_2$ and the inverse temperature $(k_B T)^{-1}$] can be written as

$$X_{\pm}(y) = \int_0^{\infty} \frac{\rho_{\pm}(y')}{y'^2 + y^2}\, dy' \tag{2.1}$$

$$= \sum_{n=0}^{\infty} \int_0^{\infty} \frac{\rho_{\pm}^{(n)}(y')}{y'^2 + y^2}\, dy' \tag{2.2}$$

$$= \sum_{n=0}^{\infty} X_{\pm}^{(n)}(y) , \tag{2.3}$$

with

$$\rho_{+}^{(2n)}(y) \equiv 0 , \qquad n = 1, 2, 3, \ldots \tag{2.4a}$$

$$\rho_{-}^{(2n-1)}(y) \equiv 0 , \qquad n = 1, 2, 3, \ldots \tag{2.4b}$$

$$\rho_{+}^{(2n-1)}(y) = \begin{cases} 0 \text{ for } y < 2n-1 \\ \text{and has no singularities for} \\ \quad y > 2n-1 , \ n = 2, 3, 4, \ldots \end{cases} \tag{2.4c}$$

$$\rho_{-}^{(2n)}(y) = \begin{cases} 0 \text{ for } y < 2n \\ \text{and has no singularities for} \\ \quad y > 2n, \ n = 1, 2, 3, \ldots \end{cases} \tag{2.4d}$$

and

$$\rho_{+}^{(1)}(y) = 2^{5/4}(\sinh 2\beta_c E_1 + \sinh 2\beta_c E_2)^{1/8}\delta(y-1) , \tag{2.4e}$$

where $E_1$ and $E_2$ are the interaction energies and $\beta_c = (k_B T_c)^{-1}$. In words, (2.1)–(2.4) mean that $X_{+}(y)$ has simple poles[27–31] at $y = \pm i$ and branch points at $y = \pm (2n+1)i$, $n = 1, 2, 3, \ldots$, and $X_{-}(y)$ has only branch points which are located at $y = \pm 2ni$, $n = 1, 2, 3, \ldots$. In Fig. 1 we qualitatively display the analytic structure of $X_{\pm}(y)$. In Fig. 2 we plot for $0 \le y \le 14$ the functions $X_{\pm}(y)/X_{\pm}(0)$. For a discussion of how to compute the infinite sum in (2.2) or (2.3) see Appendix B. Also in Appendix B in Table VIII we give the values (to at least six decimal places) of $X_{\pm}(y)/X_{\pm}(0)$. For $y > 20$ the expansion (2.10) below may be used to compute $X_{\pm}(y)$. The computation of $X_{\pm}^{(n)}(y)$ is discussed in Appendix C. In Fig. 3 we plot $X_{+}^{(3)}(y)/X_{+}^{(3)}(0)$ and the function $(1+y^2)^{-1}$ for comparison.

Many authors[32–35] have developed the connection between critical phenomena and field theory. In this language the Ising model is a Euclidean field theory, and the scale functions $X_{\pm}(y)$, which are the two-point functions, are expected to obey a dispersion relation of the form (2.1)–(2.3). [This is not to say the structure of $\rho_{\pm}^{(n)}(y)$ is that of (2.4).] This dispersion relation is expected to be valid for either the two- or three-dimensional ferromagnetic Ising model of arbitrary spin[36] and arbitrary, finite-range pairwise interactions. Thus the dispersion representation (2.1)–(2.3) represents a very general point of view in which to discuss $X_{\pm}(y)$. For this reason we discuss our computation of $X_{\pm}(y)$ for the two-dimensional (nearest-neighbor, spin-$\frac{1}{2}$) Ising model in this language.

We first reiterate the point that (2.4e) gives the

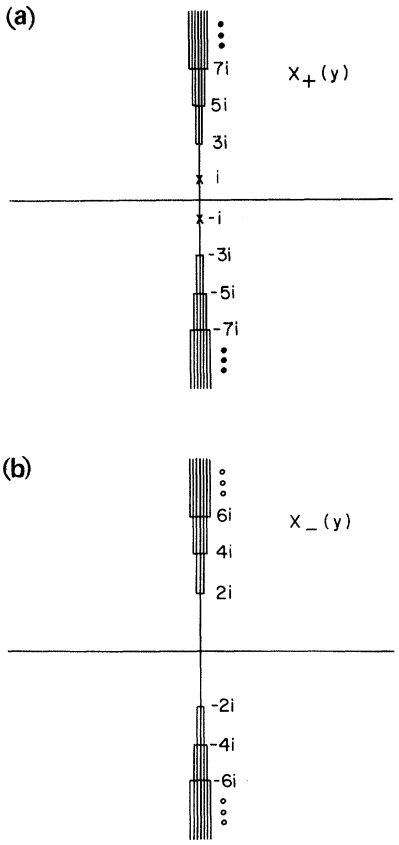


FIG. 1. (a) Analytic structure of $X_+(y)$ in the complex $y$ plane. The branch points at $\pm(2n+1)i$, $n=1,2,3,\ldots$, are square-root-type singularities, and the symbol $\times$ denotes a simple pole. The poles are the Ornstein-Zernike poles. (b) Analytic structure of $X_-(y)$ in the complex $y$ plane. $X_-(y)$ has only branch points which are located at $\pm 2ni$, $n=1,2,3,\ldots$.

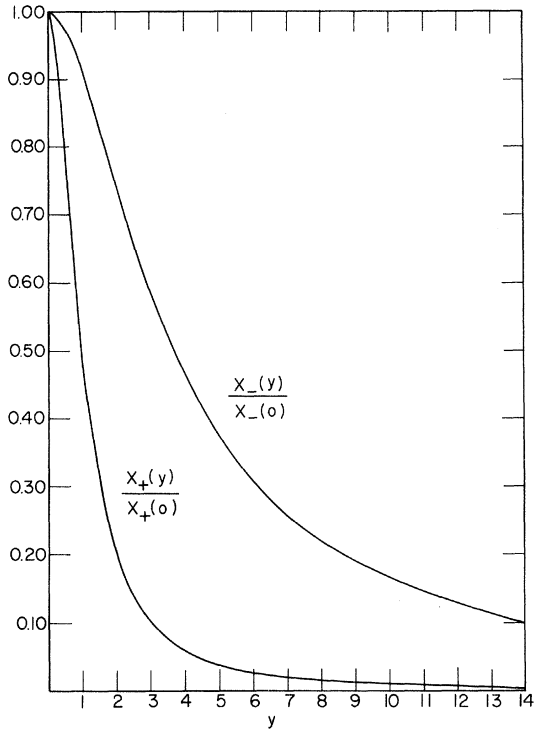


FIG. 2. Scale functions $X_\pm(y)/X_\pm(0)$ for the two-dimensional Ising model, where $X_\pm(0)$ are given in Table II.

Ornstein-Zernike pole (1.6) with

$$x_0 = 2^{5/4}(\sinh 2\beta_c E_1 + \sinh 2\beta_c E_2)^{1/8}\ .$$

In Appendix C we show that the spectral function $\rho_-^{(2)}(y)$ is given by

$$\rho_-^{(2)}(y) = \begin{cases} 0 \text{ for } y<2 \\ \dfrac{2^{5/4}}{\pi}(\sinh 2\beta_c E_1 + \sinh 2\beta_c E_2)^{1/8}\dfrac{(y^2-4)^{1/2}}{y^2} \\ \qquad \text{for } y \geq 2. \end{cases} \quad (2.5)$$

From (2.5) we see that $\rho_-^{(2)}(y)$ has a square-root branch point at $y^2=4$. In Appendix C we show that both $\rho_+^{(2n+1)}(y)$ and $\rho_-^{(2n)}(y)$, $n=1,2,3,\ldots$, display square-root-type behavior near threshold.

Using (2.5) we can compute $X_-^{(2)}(y)$, i.e., the two-particle cut contribution to the scale function $X_-(y)$:

$$X_-^{(2)}(y) = 2^{-3/4}\pi^{-1}(\sinh 2\beta_c E_1 + \sinh 2\beta_c E_2)^{1/8} \times\{(1+\tfrac{1}{4}y^2)^{1/2}(\tfrac{1}{2}y)^{-3}\ln[1+(1+\tfrac{1}{4}y^2)^{1/2}] - (\tfrac{1}{2}y)^{-2}\}. \quad (2.6)$$

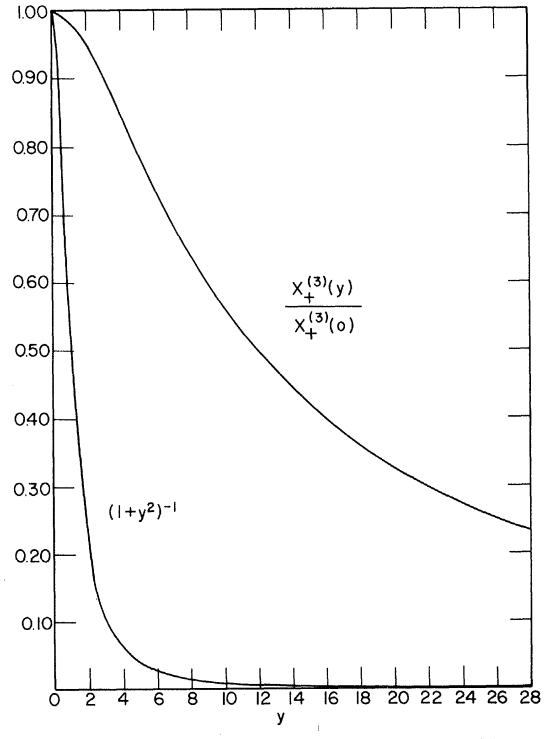


FIG. 3. Three-particle contribution $X_+^{(3)}(y)/X_+^{(3)}(0)$ to the scale function. For comparison the Ornstein-Zernike contribution $(1+y^2)^{-1}$ is also plotted.

From (2.6) for $y \to \infty$

$$X_-^{(2)}(y) = 2^{5/4}\pi^{-1}(\sinh 2\beta_c E_1 + \sinh 2\beta_c E_2)^{1/8}\frac{\ln y}{y^2} + O(y^{-2}). \tag{2.7}$$

This could have been anticipated from the fact that $\rho_-^{(2)}(y) \sim y^{-1}$ for $y \to \infty$. Using the standard convention that logarithms should be treated as a zero exponent,[3] we see the "$\eta$ assigned to $X_-^{(2)}(y)$" is zero. Of course, the same is true for the Ornstein-Zernike pole (1.6). In Appendix D we show that for $n = 1, 2, 3, \ldots$ as $y \to \infty$

$$X_+^{(2n+1)}(y) = C_{2n+1}^+ \frac{(\ln y)^{2n}}{y^2} + O\left(\frac{(\ln y)^{2n-1}}{y^2}\right) \tag{2.8}$$

and

$$X_-^{(2n)}(y) = C_{2n}^- \frac{(\ln y)^{2n-1}}{y^2} + O\left(\frac{(\ln y)^{2n-2}}{y^2}\right), \tag{2.9}$$

with $C_n^{\pm}$ constants.

*Thus if we consider only a finite sum of terms in* (2.2) [*or equivalently* (2.3)] *we will obtain a zero* $\eta$. We find that for the two-dimensional Ising model

$$X_\pm(y) = C_1 y^{-7/4}[1 \pm (C_2 \ln y + C_3)y^{-1} + C_4 y^{-2} \pm (C_5 \ln y + C_6)y^{-3} + (C_7 \ln^2 y + C_8 \ln y + C_9)y^{-4} + O(y^{-5}\ln^4 y)], \tag{2.10}$$

for $y \to \infty$. The numerical values of the coefficients $C_i$, $i = 1, 2, \ldots, 9$, are given in Table I. Analytical expressions for $C_i$, $i = 1, \ldots, 9$, along with a derivation of (2.10) can be found in Appendix D. The first term in (2.10), $C_1 y^{-7/4}$, was computed by Fisher[37] and Wu.[27] The second term in (2.10) was computed by Ryazanov[38] and by Vaks, Larkin, and Ovchinnikov[39] (however their value for $C_2$ is incorrect). The important point to emphasize is that the critical exponent $\eta$ emerges from the dispersion representation only when the entire many-particle cut structure is considered.

TABLE I. Coefficients $C_i$, $i = 1, 2, \ldots, 9$, in the large-$y$ expansion of $X_\pm(y)$ [see (2.10)] for the two-dimensional Ising model. The coefficient $C_1$ (and only $C_1$) depends upon $E_1$ and $E_2$. We give the numerical value for the symmetric lattice $E_1 = E_2$. Analytical expressions for $C_i$, $i = 1, \ldots, 9$, can be found in Appendix D.

| $i$ | $C_i$ |
|---|---|
| 1 | 1.074 999 324 29... |
| 2 | 1.606 640 946 86... |
| 3 | 0.394 857 6169... |
| 4 | −0.191 406 2500... |
| 5 | −0.759 388 8850... |
| 6 | 0.365 650 9050... |
| 7 | −0.168 228 1494 |
| 8 | −1.422 921 830... |
| 9 | 0.036 196 1956... |

TABLE II. Exact values of the scale functions $X_\pm(y)$ at $y = 0$ (for the two-dimensional symmetric Ising model) are compared with the expansion (2.3). $X_\pm^{(n)}(0)$ is the contribution to $X_\pm(0)$ coming from the $n$-particle cut.

| Exact results | Perturbation-expansion results |
|---|---|
| $X_+(0) = 2.595\,793\,633$ | $X_+^{(1)}(0) = 2^{11/8} = 2.593\,679\,109\,302\,02$ |
| | $X_+^{(3)}(0) = 0.002\,112\,454\,5415$ |
| | $X_+^{(5)}(0) = 0.000\,002\,067$ |
| | $X_+^{(1)}(0) + X_+^{(3)}(0) = 2.595\,791\,563\,843$ |
| | $X_+^{(1)}(0) + X_+^{(3)}(0) + X_+^{(5)}(0) = 2.595\,793\,631$ |
| $X_-(0) = 0.068\,865\,537\,9$ | $X_-^{(2)}(0) = 2^{11/8}(12\pi)^{-1} = 0.068\,799\,475\,173$ |
| | $X_-^{(4)}(0) = 0.000\,066\,005$ |
| | $X_-^{(2)}(0) + X_-^{(4)}(0) = 0.068\,865\,480$ |

On the other hand, the *small-y* properties of $X_\pm(y)$ are completely dominated by the lowest-lying singularities of $X_\pm(y)$. For example, the value of the scale function at the origin, $X_\pm(0)$,[11–13] which by (2.2)

$$X_\pm(0) = \sum_{n=0}^{\infty} \int_0^\infty \frac{\rho_\pm^{(n)}(y')}{y'^2}\, dy' \tag{2.11}$$

is given to a high degree of accuracy by the first few terms in (2.11). For the symmetric lattice $E_1 = E_2$ we compare in Table II the exact values of $X_\pm(0)$ (to ten significant digits) with the approximations $X_+^{(1)}(0)$, $X_+^{(1)}(0) + X_+^{(3)}(0)$, etc.

The small-$y$ expansions

$$X_-(y) = \sum_{j=0}^{\infty} R_{2j}^<(-1)^j y^{2j} \tag{2.12}$$

and

$$X_+(y) = 2^{5/4}(\sinh 2\beta_c E_1 + \sinh 2\beta_c E_2)^{1/8}(1 + y^2)^{-1} + \sum_{j=0}^{\infty} R_{2j}^>(-1)^j y^{2j} \tag{2.13}$$

are discussed in Appendix E.

The values of $R_{2j}^<$ and $R_{2j}^>$, $j = 1, 2, \ldots, 5$, for the symmetric two-dimensional Ising model are given in Table III.

One can also expand $X_\pm(y)$ for small $y$ as

TABLE III. Coefficients $R_{2j}^<$ and $R_{2j}^>$ in the small-$y$ expansions (2.12) and (2.13), respectively, for the two-dimensional symmetric Ising model.

| $j$ | $R_{2j}^<$ | $R_{2j}^>$ |
|---|---|---|
| 1 | $0.688\,0074 \times 10^{-2}$ | $0.283\,8091 \times 10^{-4}$ |
| 2 | $0.982\,850\,48 \times 10^{-3}$ | $0.832\,6690 \times 10^{-6}$ |
| 3 | $0.163\,808\,28 \times 10^{-3}$ | $0.346\,0674 \times 10^{-7}$ |
| 4 | $0.297\,833\,23 \times 10^{-4}$ | $0.175\,8059 \times 10^{-8}$ |
| 5 | | $0.101\,860\,13 \times 10^{-9}$ |

TABLE IV. Coefficients $\Sigma_{2n}^{+}$ and $\Sigma_{2n}^{-}$ for the two-dimensional Ising model [see (2.14)] are in the second and fourth columns, respectively. The estimates $\Sigma_{2n}^{FB}$ [see (3.3) and (3.8)] are in the third colum ($\Sigma_{2n}^{FB}$ should be compared with the exact $\Sigma_{2n}^{+}$). The fifth column contains the Tarko-Fisher estimates [see (3.11)], and should be compared with the exact $\Sigma_{2n}^{-}$.

| $n$ | $\Sigma_{2n}^{+}$ | $\Sigma_{2n}^{FB}$ | $\Sigma_{2n}^{-}$ | $\Sigma_{2n}^{TF}$ |
|---|---|---|---|---|
| 1 | 0.999 196 337 | 0.999 8918 | $0.999\,059\times10^{-1}$ | ... |
| 2 | $0.792\,4044\times10^{-3}$ | $0.108\times10^{-3}$ | $0.429\,0832\times10^{-2}$ | $0.420\times10^{-2}$ |
| 3 | $0.109\,3350\times10^{-4}$ | $0.526\times10^{-7}$ | $0.524\,1301\times10^{-3}$ | $0.502\times10^{-3}$ |
| 4 | $0.311\,7391\times10^{-6}$ | $0.323\times10^{-10}$ | $0.812\,396\times10^{-4}$ | |
| 5 | $0.126\,1657\times10^{-7}$ | $0.217\times10^{-13}$ | | |

$$\left(\frac{X_{\pm}(y)}{X_{\pm}(0)}\right)^{-1} = 1 + \sum_{n=1}^{\infty} (-1)^{n+1} \Sigma_{2n}^{\pm} y^{2n} . \tag{2.14}$$

Clearly the Ornstein-Zernike pole approximation corresponds to $\Sigma_2 = 1$ and $\Sigma_{2n} = 0$ for $n = 2, 3, 4, \ldots$. We find that the values of $\Sigma_{2n}^{\pm}$ are again determined to a high degree of accuracy (see Appendix E) by the lowest-lying singularities (where, of course, for $\Sigma_{2n}^{+}$ the first contribution for $n = 2, 3, \ldots$ comes from the three-particle cut). In Table IV, columns two and four, we give $\Sigma_{2n}^{\pm}$ for $n = 1, 2, \ldots, 5$. We defer comparison of these numbers with available series-expansion estimates until Sec. III.

## III. PHENOMENOLOGICAL FORMULAS FOR $X_{\pm}(y)$

### A. Ornstein-Zernike

The simplest approximate to $X_{\pm}(y)$ is the Ornstein-Zernike pole approximation

$$X_{OZ}(y) = x_0(1 + y^2)^{-1} . \tag{3.1}$$

Of course, if for $T < T_c$ there is no pole term in $X_{-}(y)$, then this will be a poor approximation. However if a pole term is present, we expect (3.1) to be an excellent approximate for small $y$. To illustrate this we compare in Table V, row 1, the Ornstein-Zernike pole approximate (3.1) (with $x_0 = 1$) with the exact $X_{+}(y)/X_{+}(0)$ for the two-dimensional Ising model. One sees that to within 5% accuracy the simple pole gives $X_{+}(y)/X_{+}(0)$ in the range $0 \le y \le 11.2$. Thus even though $\eta = \frac{1}{4}$ is considered large, the Ornstein-Zernike pole approximation is quite good over a large range of $y$, i.e., $y \le 11$. Note that for $y = 11$ the scale function $X_{+}(y)/X_{+}(0)$ is only 0.86% of its value in the forward direction $y = 0$. Stated slightly differently we conclude that any experiment that wants to measure $\eta$ must be in a region of $y$ where the pole term does not dominate.

The fact that the coefficients $\Sigma_{2n}^{+}$, $n = 2, 3, \ldots$, in (2.14) are small (see Table IV) is somewhat of an indication of the dominance of the pole term for small $y$. The reason we say "somewhat" is that the expansion (2.14) does not converge for $y \ge 3$ for $X_{+}(y)$.

In the x-ray scattering studies of argon for $T > T_c$ by Lin and Schmidt,[24] these authors scale their data and find that $y$ must be greater than 12 to find significant (i.e., greater than could be accounted for by uncertainties in the intensity measurements) deviations from Ornstein-Zernike.

### B. Fisher approximate

The Fisher approximate[2] is

$$X_F(y) = A(1 + y^2)^{-1+\eta/2} . \tag{3.2}$$

The constant $A$ can be chosen to reproduce either $X_{\pm}(0)$ or to reproduce the leading term of the large-$y$ expansion of $X_{\pm}(y)$, in which case $A$ is set equal to $C_1$ of (1.9). To do this one must have an independent method of determining either $X_{\pm}(0)$ or $C_1$. The analytic structure of $X_F(y)$ consists of two branch points at $y = \pm i$.

If we set $A = 1$ and compare $X_F(y)$ with $X_{+}(y)/X_{+}(0)$, we find the deviations exceed 5% for $y > 0.7$. Setting $A$ equal to the known value of $C_1$ (see Table I), then in Table V, row 2, we compare $X_F(y)$ with $X_{\pm}(y)$. Note that $y$ must exceed 163 for $X_F(y)$ to reproduce $X_{+}(y)$ to within an accuracy of 5%. No experiments at present[14-24] can reach such a high value of $y$.

### C. Fisher-Burford approximate

The Fisher approximate (3.2) can be made to match the leading term of the large-$y$ behavior of $X_{+}(y)$, but not the correct small-$y$ behavior. To overcome this objection, Fisher and Burford[5] proposed the following approximate:

$$X_{FB}(y) = A \frac{(1 + \phi_c^2 y^2)^{\eta/2}}{1 + y^2} \tag{3.3}$$

for scale functions [such as $X_{+}(y)$] that have a pole. The constant $A$ is determined by requiring

$$A = X_{+}(0) \tag{3.4}$$

and the constant $\phi_c$ is determined by requiring that (3.3) reproduce the leading term of the large-$y$ expansion of $X_{+}(y)$, i.e.,

$$A\phi_c^{\eta} = C_1 , \tag{3.5}$$

where $C_1$ is given by (1.9).

For the two-dimensional Ising model $\phi_c$ can be determined *exactly*,

$$\phi_c = 0.029\,413\,86\ldots . \tag{3.6}$$

The careful reader will have noted that what we call the Fisher-Burford approximate, i.e., (3.3), is slightly different than that in Fisher and Burford.[5] The difference is due to the different definitions of the scale variable. Here we let $y = k\xi$, with $\xi$ the exact correlation length (see Appendix A for details). Fisher and Burford let $x = k\xi_1$, with

TABLE V. This table compares the exact scale functions $X_{\pm}(y)$ for the two-dimensional Ising model with various approximate scale functions. The various approximates are given in the left-hand column (see text for definitions). The approximates $X_{OZ}(y)$, $X_F(y)$, $X_{FB}(y)$, $(1+\Sigma_2^{\pm}y^2-\Sigma_4^{\pm}y^4)^{-1}$, $(1+\Sigma_2^{\pm}y^2-\Sigma_4^{\pm}y^4+\Sigma_6^{\pm}y^6)^{-1}$, $X_-^{(2)}(y)/X_-^{(2)}(0)$, $X_{TF}^{(1)}(y)$, and $X_{TF}^{(2)}(y)$ are all normalized to unity at $y=0$, and hence, are compared with the scale functions $X_{\pm}(y)/X_{\pm}(0)$. The error in percent is defined as the exact value minus the approximate value, divided by the exact value. The upper row gives the error. Thus, for instance, the Fisher-Burford approximate $X_{FB}(y)$ agrees with the exact $X_+(y)/X_+(0)$ to within 0.1% over the ranges $0 \le y < 1.1$ and $15\,900 < y < \infty$. The second column specifies if the comparison is with the scale function $X_+(y)$ $(T > T_c)$ or with the scale function $X_-(y)$ $(T < T_c)$. Three dots indicate that this region was not determined. The last row gives the comaprison of the Fisher-Burford approximate $X_{FB}(y)$ with the parameters $\phi_c$, $\eta$, and $X_{FB}(0)$ determined by a least-squares program with the exact $X_+(y)$ (see Sec. IV for discussion).

| Approx. | | Error 0.01% | 0.1% | 1% | 5% | 10% |
|---|---|---|---|---|---|---|
| $X_{OZ}(y)$ | $T>T_c$ | $0 \le y < 0.3$ | $0 \le y < 1.1$ | $0 \le y < 4.0$ | $0 \le y < 11.2$ | $0 \le y < 21$ |
| | $T<T_c$ | ... | ... | $0 \le y < 0.1$ | $0 \le y < 0.2$ | $0 \le y < 0.3$ |
| $X_F(y)$ | $T>T_c$ | $200\,000 < y < \infty$ | $15\,900 < y < \infty$ | $1170 < y < \infty$ | $163 < y < \infty$ | $64 < y < \infty$ |
| | $T<T_c$ | $200\,000 < y < \infty$ | $15\,900 < y < \infty$ | $1185 < y < \infty$ | $185 < y < \infty$ | $80 < y < \infty$ |
| $X_{FB}(y)$ | $T>T_c$ | $0 \le y < 0.3$<br>$200\,000 < y < \infty$ | $0 \le y < 1.1$<br>$15\,900 < y < \infty$ | $0 \le y < 4.2$<br>$1145 < y < \infty$ | $0 \le y < 15$<br>$138 < y < \infty$ | $0 \le y < \infty$ |
| $(1+\Sigma_2^{\pm}y^2-\Sigma_4^{\pm}y^4)^{-1}$ | $T>T_c$ | $0 \le y < 0.3$ | $0 \le y < 3.8$ | $0 \le y < 6.6$ | $0 \le y < 10.8$ | $0 \le y < 13.8$ |
| | $T<T_c$ | $0 \le y < 0.8$ | $0 \le y < 1.1$ | $0 \le y < 1.9$ | $0 \le y < 2.5$ | $0 \le y < 3$ |
| $(1+\Sigma_2^{\pm}y^2-\Sigma_4^{\pm}y^4+\Sigma_6^{\pm}y^6)^{-1}$ | $T>T_c$ | $0 \le y < 0.3$ | $0 \le y < 3.4$ | $0 \le y < 6.4$ | $0 \le y < 9.2$ | $0 \le y < 11$ |
| | $T<T_c$ | $0 \le y < 1.1$ | $0 \le y < 1.5$ | $0 \le y < 2.1$ | $0 \le y < 2.6$ | $0 \le y < 2.9$ |
| $X_{OZ}(y)+X_+^{(3)}(y)$ | $T>T_c$ | $0 \le y < 12$ | $0 \le y < 40$ | $0 \le y < 250$ | $0 \le y < 1500$ | ... |
| $C_1 y^{-7/4}$ | $T>T_c$ | $200\,000 < y < \infty$ | $15\,900 < y < \infty$ | $1170 < y < \infty$ | $163 < y < \infty$ | $64 < y < \infty$ |
| | $T<T_c$ | $200\,000 < y < \infty$ | $15\,900 < y < \infty$ | $1170 < y < \infty$ | $184 < y < \infty$ | $82 < y < \infty$ |
| $X_{FL}^{\pm}(y)$ | $T>T_c$ | $47 < y < \infty$ | $15.7 < y < \infty$ | $5.4 < y < \infty$ | $2.5 < y < \infty$ | $1.7 < y < \infty$ |
| | $T<T_c$ | $40 < y < \infty$ | $12.4 < y < \infty$ | $5.5 < y < \infty$ | $3.6 < y < \infty$ | $3 < y < \infty$ |
| Large-$y$ Expansion (2.10) | $T>T_c$ | $5.5 < y < \infty$ | $3.5 < y < \infty$ | $1.5 < y < \infty$ | $1.2 < y < \infty$ | $1.1 < y < \infty$ |
| | $T<T_c$ | $6.7 < y < \infty$ | $3.5 < y < \infty$ | $2.7 < y < \infty$ | $2.1 < y < \infty$ | $1.9 < y < \infty$ |
| $\frac{X_-^{(2)}(y)}{X_-^{(2)}(0)}$ | $T<T_c$ | $0 \le y < 1.1$ | $0 \le y < 3.8$ | $0 \le y < 19$ | $0 \le y < 102$ | $0 \le y < 287$ |
| $X_{TF}^{(1)}(y)$ | $T<T_c$ | $0 \le y < 0.1$<br>$146\,000 < y < \infty$ | $0 \le y < 0.3$<br>$10\,350 < y < \infty$ | $0 \le y < 1.2$<br>$585 < y < \infty$ | $0 \le y < 4.1$<br>$45 < y < \infty$ | $0 \le y < \infty$ |
| $X_{TF}^{(2)}(y)$ | $T<T_c$ | $0 \le y < 0.3$ | $0 \le y < 1.0$ | $0 \le y < 4.8$<br>$260 < y < \infty$ | $0 \le y < \infty$ | $0 \le y < \infty$ |
| $X_{FB}(y)$ with LSV[a] | $T>T_c$ | not attainable | $17.5 < y < 51$ | $8.8 < y < 103$ | $0 \le y < 310$ | $0 \le y < 800$ |

[a]Least-squares value.

$\xi_1$ the second-moment definition of the correlation length. The second-moment definition is such that the second term in the inverse expansion (2.14) in terms of the $x$ variable is always $x^2$. Hence the connection between our $y$ and the $x$ variable is

$$\Sigma_2^{\pm} y^2 = x^2 , \tag{3.7}$$

where one uses $\Sigma_2^+$ ($\Sigma_2^-$) above (below) $T_c$.

Comparing the analytic structure of $X_{FB}(y)$ with $X_+(y)$ [see Fig. 1(a)] we see that $X_{FB}(y)$ has replaced the infinite sequence of square-root branch points at $y = \pm i(2n+1)$, $n = 1, 2, 3, \ldots$, with a single branch point of order $\eta/2$ at $y = \pm i\phi_c^{-1}$. Also comparing the large-$y$ expansion of $X_{FB}(y)$ with the exact large-$y$ expansion of $X_+(y)$ [see (2.10)], we see that $X_{FB}(y)$ does not reproduce, other than the leading term, the correct large-$y$ behavior [the same remark holds for the Fisher approximate (3.2)]. In Sec. IV this deficiency of (3.2) and (3.3) will be crucial in understanding why many experiments that use either the Fisher or the Fisher-Burford approximate in the data analysis for determin-

ing the exponent $\eta$ are in serious doubt.

In Table V, row 3, we compare $X_{FB}(y)$ of (3.3) with $A=1$ and $\phi_c$ given by (3.6) with $X_+(y)/X_+(0)$. To within 10% accuracy, $X_{FB}(y)$ reproduces $X_+(y)/X_+(0)$ for all $y$. To within 5% accuracy $X_{FB}(y)$ is slightly better than Ornstein-Zernike for small $y$, but for large $y$ one does not obtain this accuracy until $y>138$.

One can also use (3.3) with the exactly known $\phi_c$ to obtain estimates for the coefficients $\Sigma_{2n}^+$ of (2.14). From (3.3) it follows that

$$\Sigma_{2k}^{FB}=[(k-1)!]^{-1}\frac{\eta}{2}\left(\frac{\eta}{2}+1\right)\cdots \times\left(\frac{\eta}{2}+k-2\right)\phi_c^{2k-2}\left[1-k^{-1}\left(\frac{\eta}{2}+k-1\right)\phi_c^2\right]. \quad (3.8)$$

Using $\eta=\frac{1}{4}$ and $\phi_c$ given by (3.6) we obtain from (3.8) the Fisher-Burford estimates for the coefficients $\Sigma_{2n}^+$ for the two-dimensional Ising model. For $n=1,\ldots,5$ we give the numerical value of $\Sigma_{2n}^{FB}$ in column 3 of Table IV. These estimates should be compared with the exact $\Sigma_{2n}^+$ in column 2, Table IV.

### D. Approximates $(1+\Sigma_2^\pm y^2-\Sigma_4^\pm y^4)^{-1}$ and $(1+\Sigma_2^\pm y^2-\Sigma_4^\pm y^4+\Sigma_6^\pm y^6)^{-1}$

Using the known values of $\Sigma_2^\pm$, $\Sigma_4^\pm$, and $\Sigma_6^\pm$ (see Table IV) we compare the approximates $(1+\Sigma_2^\pm y^2-\Sigma_4^\pm y^4)^{-1}$ and $(1+\Sigma_2^\pm y^2-\Sigma_4^\pm y^4+\Sigma_6^\pm y^6)^{-1}$ with $X_\pm(y)/X_\pm(0)$ in Table V, rows 4 and 5, respectively.

### E. $X_{OZ}(y)+X_+^{(3)}(y)$

Though the contribution to $X_+(y)$ from the three-particle cut is expressed in integral form in Appendix C, we can evaluate this integral numerically and compare $X_+(y)$ with the sum of the Ornstein-Zernike pole and the three-particle cut contribution. In Table V, row 6, we give this comparison. The three dots indicate that we did not determine this region of accuracy. One sees the rather surprising result that $X_+(y)$ and $X_{OZ}(y)+X_+^{(3)}(y)$ agree to within 0.1% in the region $y$ less 40. It is interesting to note that $X_+^{(3)}(y)$ is only 4.6% (10.6%) of $X_{OZ}(y)$ at $y=10$ (20). We find that $X_+^{(3)}(y)=X_{OZ}(y)$ when $y\sim 542$.

### F. $y^{-2+\eta}$ approximate

Since (by definition) $X_\pm(y)$ approaches $C_1y^{-2+\eta}$ as $y\to\infty$, there is a region of sufficiently large $y$ where it is possible to replace $X_\pm(y)$ by $C_1y^{-2+\eta}$. For the two-dimensional Ising model Table V, row 7, shows that this region is for $y$ quite large. For example, for $C_1y^{-7/4}$ to give $X_\pm(y)$ to within 1% accuracy $y$ must be greater than 1170.

### G. Fisher-Langer approximate

When $y^{-2+\eta}$ is not a good approximation (and we expect this to be the case for all present experimental work) and $y\gg 1$, we must consider corrections to the leading-order term in the large-$y$ expansion of $X_\pm(y)$. Fisher[40] and Fisher and Langer[25] have argued that for $y\to\infty$

$$X_\pm(y)\sim C_1y^{-2+\eta}(1\pm C_2y^{-(1-\alpha)/\nu}+C_3^\pm y^{-1/\nu}), \quad (3.9)$$

with $\alpha$ the critical exponent describing the divergence of the specific heat, $\nu$ is defined by (1.3), and $C_2$ and $C_3^\pm$ are constants with $C_2$ being non-negative. For the two-dimensional Ising model $\nu=1$ and $y^{\alpha/\nu}$ is replaced by $\ln y$ [see (2.10)]. The form (3.9), which we call the Fisher-Langer approximate, has more recently been discussed by Stell,[41] by Polyakov,[31] by Fisher and Aharony,[7] where the coefficients $C_i$ have been computed to order $\epsilon^2$ using the $\epsilon$-expansion techniques of Wilson and Fisher,[43] by Brézin, Amit, and Zinn-Justin,[44] and by Brézin, Guillou, and Zinn-Justin.[44] Hocken and Stell[42] (see also Ref. 44) show that the ratio $C_3^+/C_3^-$ is the negative of the ratio of the specific-heat amplitudes above and below $T_c$. For the two-dimensional Ising model the third term in (2.10) is a special case of this result.

For the two-dimensional Ising model we compare in Table V, row 8, the Fisher-Langer approximate (3.9) (with $\nu=1$, $y^{\alpha/\nu}\to\ln y$, and the coefficients $C_1$, $C_2$, and $C_3$ given in Table I) with the exact scale functions $X_\pm(y)$. For all $y>5.5$ the Fisher-Langer approximate (3.9) agrees with the exact scale functions $X_\pm(y)$ to within an accuracy of 1%.

We plot in Fig. 4 the quantity $(C_2\ln y+C_3)y^{-1}$ to illustrate the importance of this term relative to the leading-order term $C_1y^{-7/4}$. We see, for example, that at $y\simeq 20$ the correction terms in the Fisher-Langer approximate are of the order of 25% of the term $C_1y^{-7/4}$.

In Table V, row 9, we compare the large-$y$ expansion (2.10) with the exact scale functions $X_\pm(y)$. For all $y>6.7$ the expansion (2.10) reproduces the exact scale functions $X_\pm(y)$ to within an accuracy of 0.01%. It is interesting to compare the overlap of the pole term (above $T_c$) and the large-$y$ expansion (2.10).

### H. $X_-^{(2)}(y)$

Below $T_c$ in the two-dimensional Ising model the lowest-lying singularity is a two-particle cut. In Table V, row 10, we compare $X_-(y)/X_-(0)$ and $X_-^{(2)}(y)/X_-^{(2)}(0)$ [see (2.6)]. To within 1% accuracy the two-particle cut contribution to $X_-(y)$ reproduces $X_-(y)$ for all $y\leq 19$.

### I. Tarko-Fisher approximates

Tarko and Fisher[8] have proposed two approximates for the scale function $X_-(y)$ (and specifically for the two-dimensional Ising model). The first approximate is

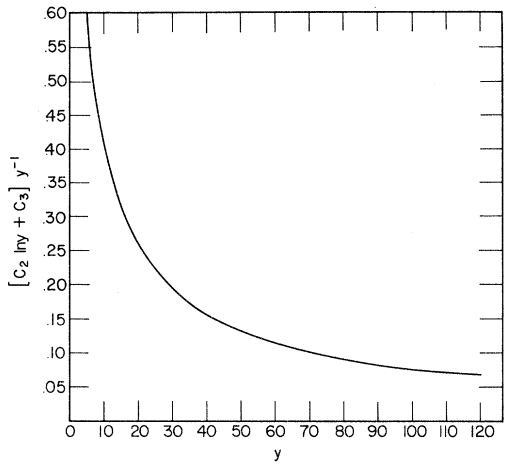


FIG. 4. Quantity $(C_2 \ln y + C_3)y^{-1}$, where the coefficients $C_2$ and $C_3$ are given in Table I.

$$X_{\mathrm{TF}}^{(1)}(y) = A[1 - p + p(1 + y^2/4)^{1/2}]^{-(2-\eta)} \tag{3.10}$$

and the second approximate is

$$X_{\mathrm{TF}}^{(2)}(y) = A\,\frac{(1+\phi^2 y^2)^{\eta/2}}{[1 - \lambda + \lambda(1 + y^2/4)^{1/2}]^2}\ . \tag{3.11}$$

In both (3.10) and (3.11) the square-root factor $(1+y^2/4)^{1/2}$ is introduced to produce the known location of the square-root branch point $y = \pm 2i$ [see (2.6)]. In both (3.10) and (3.11) the constant $A$ is chosen so that $X_{\mathrm{TF}}(0) = X_-(0)$.

In (3.10) we determine $p$ by requiring that the large-$y$ expansion of (3.10) reproduces the leading term of the large-$y$ expansion of $X_-(y)$ [see (2.10)], i.e.,

$$C_1 = A(\tfrac{1}{2}p)^{-2+\eta}\ . \tag{3.12}$$

Since we know $\eta$ and $C_1$ for the two-dimensional Ising model we can *exactly* compute $p$,

$$p = 0.415\,9906\ldots\ . \tag{3.13}$$

We compare in Table V, row 11, (3.10) [$A=1$ and $p$ given by (3.13)] with $X_-(y)/X_-(0)$.

In the second Tarko-Fisher approximate (3.11) $\phi$ and $\lambda$ are determined by requiring that the small-$y$ expansion of (3.11) reproduce exactly the coefficient $\Sigma_2^-$ of (2.14), i.e.,

$$\Sigma_2^- = \tfrac{1}{4}\lambda - \tfrac{1}{2}\eta\phi^2\ , \tag{3.14}$$

and the large-$y$ expansion of (3.11) reproduce exactly the leading-order term $C_1 y^{-7/4}$, i.e.,

$$C_1 = A4\phi^{\eta}/\lambda^2\ . \tag{3.15}$$

If we now use the exactly known values $\eta = \frac{1}{4}$, $A = X_-(0) = 0.068\,865\,5379\ldots$, $\Sigma_2^- = 0.099\,9059\ldots$, and $C_1 = 1.074\,999\,32\ldots$, then we find that (3.14) *and* (3.15) *have no real solution.* That is there are no real values of $\lambda$ and $\phi$ given the exact information $X_-(0)$, $\Sigma_2^-$, and $C_1$ that will satisfy both (3.14) and (3.15).

However, one can "almost" satisfy (3.14) and (3.15) by taking

$$\phi \simeq 0.20 \tag{3.16a}$$

and

$$\lambda \simeq 0.45\ . \tag{3.16b}$$

As a check on (3.16) we use these of values of $\lambda$ and $\phi$ to predict a $\Sigma_2^- = 0.0987\ldots$ and $C_1/X_-(0) = 15.5\ldots$ (as compared to $15.610\,20\ldots$).

Using (3.16) in (3.11) we compute the Tarko-Fisher approximate and compare this with $X_-(y)$. We give the results in Table V, row 12. The Tarko-Fisher approximate (3.11) with $A=1$ and the values (3.16) reproduce $X_-(y)/X_-(0)$ to within 3% for all values of $y$.

We can also use (3.11) to estimate the coefficients $\Sigma_{2n}^-$ in the expansion (2.14) of $X_-(y)$. Expanding (3.11) and using $\eta = \frac{1}{4}$ and the values (3.16) we obtain the Tarko-Fisher estimates $\Sigma_{2n}^{\mathrm{TF}}$ for $n \geq 2$. We give $\Sigma_4^{\mathrm{TF}}$ and $\Sigma_6^{\mathrm{TF}}$ in Table IV, column 5. They compare quite well with the exact values.

Tarko and Fisher[8] by use of series-expansion techniques give the estimate $\Sigma_4^- \simeq 0.13 \times 10^{-2}$. One sees that the series-expansion result is in considerable error.

## IV. CRITICAL SCATTERING AND THE EXPONENT $\eta$

### A. Scaling the experimental data

Though the scaling hypothesis[1,2] (1.5) has been known for some time, most authors[14–23] do not attempt to scale their scattering data. Clearly for $T > T_c$ and near the critical point the scattering sufficiently close to the forward direction ($k\xi < 1$) can be fit by the Ornstein-Zernike pole approximation (3.1) of (1.5). Using this three-parameter fit (the parameters are $\nu$, $\xi_0$, and the normalization constant $x_0$) the correlation length $\xi$, and hence the scale variable $y = k\xi$, can then be determined. Once $y$ is determined one can then test the scaling hypothesis (1.5) for larger values of $y$. Since the pole term always scales, it is in the large-$y$ region that any breakdown of scaling will occur. We strongly recommend that all data be presented in scale-variable and scale-function language.

### B. $\eta$ and $\tilde{\eta}$

Once one has determined $\nu$ (and the scale variable $y$), then a natural candidate for the exponent $\eta$ is

$$\tilde{\eta} \equiv 2 - \gamma/\nu\ . \tag{4.1}$$

That is, scaling will be true if $\eta$ as defined by (1.9) is such that

$$\eta = \tilde{\eta} \tag{4.2}$$

so that

$$\gamma=(2-\eta)\nu\ . \tag{4.3}$$

It is instructive to compare $\eta$ and $\tilde{\eta}$ not in $k$ space, but rather in coordinate space. Here the spin-spin correlation function $\langle\sigma_0\sigma_{\vec{R}}\rangle$ is expected from the scaling hypothesis[1,2] to be of the form

$$\langle\sigma_0\sigma_{\vec{R}}\rangle=\frac{F_\pm(t)}{R^{d-2+\eta}}+o(R^{-d+2-\eta}) \tag{4.4a}$$

as

$$R\to\infty\ ,\qquad T\to T_c^\pm\ , \tag{4.4b}$$

such that

$$t=R/\xi \tag{4.4c}$$

is fixed. For the quantity $\eta$ in (4.4a) ($d$ is the dimensionality) to be equivalent to the critical exponent $\eta$ defined by (1.9) we must have

$$F_+(0)=F_-(0)\neq 0\ . \tag{4.5}$$

Statement (4.5) is the crucial statement.

Now suppose that we examine the correlation function *away* from $T=T_c$, and scale all variables according to (4.4c); then away from $T=T_c$ (that is, $t\to\infty$) we observe, say, that the correlation function $\langle\sigma_0\sigma_{\vec{R}}\rangle$ "scales" as

$$\langle\sigma_0\sigma_{\vec{R}}\rangle=\frac{\tilde{F}_\pm(t)}{R^{d-2+\tilde{\eta}}}+o(R^{-d+2-\tilde{\eta}})\ . \tag{4.6}$$

That is, $\tilde{\eta}$ is determined by scaling the correlation function $\langle\sigma_0\sigma_{\vec{R}}\rangle$ far ($t\to\infty$) from the critical point. To verify that $\tilde{F}_\pm(t)$ is the actual scaling function $F_\pm(t)$ we must show that $\lim_{t\to 0}\tilde{F}_\pm(t)\neq 0$. The scaling hypothesis says that this will be the case if when we scale the correlation function $\langle\sigma_0\sigma_{\vec{R}}\rangle$ we include all $O(1)$ terms [$O(1)$ with respect to $R^{-d+2-\tilde{\eta}}$]. As an example of how Ornstein-Zernike fails the scaling condition (4.5) in the two-dimensional Ising model we present the following example. Suppose that when we scale we include only the terms of order $e^{-t}$ (that is, we neglect all terms of order $e^{-2t}, e^{-3t}, \ldots$). Then for the two-dimensional Ising model one would obtain

$$\tilde{\eta}=\tfrac{1}{4}\ , \tag{4.7}$$

and for the symmetric lattice for $\tilde{F}_+(t)$ the result[13]

$$\tilde{F}_+(t)=2^{3/8}\pi^{-1}t^{1/4}K_0(t)\ , \tag{4.8}$$

where $K_0(t)$ is the modified Bessel function of zeroth order, and $t$ is given by (4.4c). Now since $K_0(t)\sim-\ln t$ as $t\to 0$ we see that

$$\lim_{t\to 0}\tilde{F}_+(t)=0\ . \tag{4.9}$$

Thus if $\tilde{F}_+(t)$ [as defined by (4.8)] were the actual $F_+(t)$ for the two-dimensional Ising model, then the scaling condition (4.5) would fail. However, from a numerical point of view how easy (or hard) is (4.9) to see? In Fig. 5 we plot $\tilde{F}_+(t)$ as defined by (4.8) and the actual $F_+(t)$ for the two-dimensional Ising model. One sees from Fig. 5 that $\tilde{F}_+(t)$ doesn't "turn over" until $t\simeq 0.019$, and so, one has no indication that $\lim_{t\to 0}\tilde{F}_+(t)=0$ until one is in the range $t\leq 0.019$.

As one considers the contribution to $\tilde{F}_+(t)$ from the $e^{-3t}, e^{-5t}, \ldots$ terms the position of the maximum of $\tilde{F}_+(t)$ moves toward the origin and still (4.7) and (4.9) hold, until the infinite sum of terms gives the correct $F_+(t)$ with $F_+(0)\neq 0$.

### C. Least-squares "experiment"

In Sec. III we discussed several phenomenological formulas for $X_\pm(y)$. Here we use our six-place values of $X_\pm(y)$ as "data" over various ranges of $y$ and try by using various phenomenological formulas to extract the critical exponent $\eta$. As was made clear in Sec. III, the pole term is so dominant in the region $y<10$ that one should not use data from this region in attempting to extract $\eta$. For instance, if one uses the Fisher approximate $X_F(y)$ [see (3.2)] to fit the data in the range $0\leq y\leq 10$, then a least-squares fitting program gives $\eta\simeq 0.02$.

In Table VI we present our results. Basically no more need be said; however, we make a few comments. For example, for 100 data points over the range $20\leq y\leq 60$, $X_F(y)$ gives $\eta\simeq 0.13$ and $X_{FB}(y)$ [see (3.3)] gives $\eta=0.18$. There is no real difference between the Fisher approximate and the $y^{-2+\eta}$ approximate. The Fisher-Burford approximate fits the data quite well in the sense that the computed values from the fitted $X_{FB}(y)$ reproduce the exact input values of $X_+(y)$ to three significant figures. In Table V, row 13, the Fisher-Burford approximate $X_{FB}(y)$ with the values $\eta=0.175635$, $\phi_c=0.057098$, and $A=2.668\,69$ [these parameters were determined from a least-squares fit of $X_{FB}(y)$ to 100 values of $X_+(y)$ equally spaced and equally weighted over the interval $20<y<60$] are compared

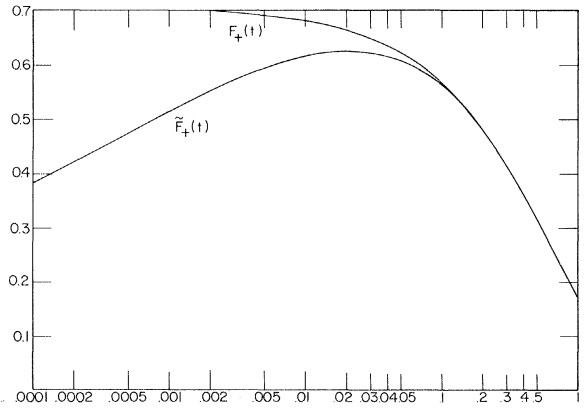


FIG. 5. Function $\tilde{F}_+(t)=\pi^{-1}2^{3/8}t^{1/4}K_0(t)$ and the scale function $F_+(t)$ as functions of $t=R/\xi$.

TABLE VI. This table gives the predicted critical exponent $\eta$ from a least-squares fit to a phenomenological formula. The formulas are given in the left-hand column (see text for definitions). The upper row gives the interval over which the formula was fitted. The number of data points, which are equally spaced and equally weighted, is also given. The second column specifies if the data are above or below $T_c$.

| Approximate | | (10,30) 50 points | (10,50) 100 points | (20,40) 50 points | (20,60) 100 points | (20,80) 150 points | (20,100) 200 points | (20,140) 300 points | (20,200) 450 points |
|---|---|---|---|---|---|---|---|---|---|
| Fisher approx. $X_F(y)$ | $T>T_c$ | 0.086[a] | 0.094 | 0.123 | 0.131[a] | 0.136[a] | 0.138[a] | 0.142[a] | 0.144[a] |
| | $T<T_c$ | 0.544[a] | 0.514[a] | 0.441[a] | 0.421[a] | 0.411[a] | 0.405[a] | 0.397[a] | 0.392[a] |
| Fisher-Burford approx. $X_{FB}(y)$ | $T>T_c$ | 0.143 | 0.154 | 0.168 | 0.176 | 0.180 | 0.184 | 0.188 | 0.191[a] |
| $C_1 y^{-2+\eta}$ | $T>T_c$ | 0.095[a] | 0.102[a] | 0.125 | 0.133[a] | 0.137[a] | 0.140[a] | 0.143[a] | 0.145[a] |
| | $T<T_c$ | 0.551[a] | 0.519[a] | 0.443[a] | 0.423[a] | 0.413[a] | 0.406[a] | 0.399[a] | 0.393[a] |
| Fisher-Langer $C_1 y^{-2+\eta}+C_2(\ln y)y^{-3+\eta}$ | $T>T_c$ | 0.299[a] | 0.281 | 0.264 | 0.260 | 0.258 | 0.258 | 0.256 | 0.256 |
| | $T<T_c$ | 0.228 | 0.233 | 0.241 | 0.243 | 0.244 | 0.244 | 0.245 | 0.245 |
| Fisher-Langer $C_1 y^{-2+\eta}+(C_2\ln y+C_3)y^{-3+\eta}$ | $T>T_c$ | 0.256 | 0.253 | 0.2510 | 0.2507 | 0.2506 | 0.2505 | 0.2504 | 0.2504 |
| | $T<T_c$ | 0.251 | 0.251 | 0.2501 | 0.2501 | 0.2501 | 0.2501 | 0.2501 | 0.2501 |
| $C_1 y^{-2+\eta}+By^{-3+\eta}[(y^\lambda-1)/\lambda]$ | $T<T_c$ | 0.248 | 0.248 | 0.247 | 0.247 | 0.248 | 0.248 | 0.248 | 0.248 |
| | $T<T_c$ | 0.268 | 0.264 | 0.257 | 0.255 | 0.255 | 0.254 | 0.253 | 0.253 |
| Tarko-Fisher $X_{TF}^{(1)}(y)$ | $T<T_c$ | 0.294 | 0.289 | 0.282 | 0.278 | 0.276 | 0.275 | 0.273 | 0.272 |
| Tarko-Fisher $X_{TF}^{(2)}(y)$ | $T<T_c$ | 0.235 | 0.237 | 0.232 | 0.268 | 0.268 | 0.234 | 0.264 | 0.263 |

[a]Some of the fitted values differ from the input values by 1% or more.

with the exact $X_+(y)$. The fit is excellent over experimentally accessible $y$, but the predicted $\eta$ is in approximately 30% error.

The reason for these large errors is that $X_F(y)$ and $X_{FB}(y)$ are not really valid in the range of experimentally accessible $y$. The "$\eta$" appearing in these formulas is the true $\eta$ from a least-squares-fitting point of view only when $y^{-2+\eta}$ is a good approximation. As we have discussed in Sec. III, this is not the case in the region $y<1000$. Instead one must use the Fisher-Langer approximate [see (3.9)]. Using (3.9) with the same data over the range $20<y<60$ with $y^{\alpha/\nu}\to \ln y$ and $C_3\to 0$ we find from a least-squares fit an $\eta$ with only 4% error. If we use (3.9) with $\nu=1$ and, say $C_2=C_3$, then the fitting program gives an equally good $\eta$ and $\alpha = -0.069$.

It should also be noted that for the second Tarko-Fisher approximate the values of $\eta$ are both above and below $\frac{1}{4}$. This variation is not seen in any oth-

TABLE VII. Experimental results for the critical exponent $\eta$. The third column gives the phenomenological formula used in the data analysis. The last column gives the reference to this work.

| System | Incident beam | Phenomenological formula | $\eta$ | Ref. |
|---|---|---|---|---|
| DAG[a] | neutrons | Fisher approx. | $0.12\pm0.1$ | 14 |
| $MnF_2$ | neutrons | Fisher approx. | $0.05\pm0.02$ | 15 |
| $RbMnF_3$ | neutrons | Fisher approx. and $k^{-2+\eta}$ approx. | $0.055\pm0.01$ | 16 |
| $K_2NiF_4$ | neutrons | Fisher-Burford approx. | $0.4\pm0.1$ | 17 |
| $CO_2$ | light | $(2-\eta)\nu=\gamma$ assumed | $0.074\pm0.035$ | 18 |
| neon | neutrons | $k^{-2+\eta}$ approx. | $0.11^{+0.03}_{-0.02}$ | 19 |
| $K_2CoF_4$ | neutrons | Fisher approx. | $0.2\pm0.1$ | 20 |
| $MnTiO_3$ | neutrons | Fisher approx. | $0.2\pm0.15$ | 21 |
| argon | x-ray | Fisher-Burford and $(2-\eta)\nu=\gamma$ assumed | $0.1\pm0.05$ | 22 |
| $\beta$-brass | neutrons | $(2-\eta)\nu=\gamma$ assumed | $0.077\pm0.067$ | 23 |

[a]Dysprosium aluminum garnet.

er approximate and is presumably related to the fact that (3.14) and (3.15) have no real solution.

### D. Experimental results for $\eta$

Many experiments[14–23] have reported measurements of $\eta > 0$, and we have summarized these results in Table VII. Those experiments[18,22,23] that assume $(2-\eta)\nu = \gamma$ in their analysis are clearly not providing an independent measurement of $\eta$. The fact that these authors show that $2\nu \neq \gamma$ is just showing that $\tilde{\eta}$ [see (4.1)] is not zero. The remaining cases use either the Fisher, Fisher-Burford, or the $k^{-2+\eta}$ approximate in the data analysis.

The first difficulty one has in assessing these experiments is the absence of any test to ensure that the data used is in the critical region, that is to say, any test to ensure that the data scales. However, if we *assume* here that all data used is in the scaling region, then the largest values of $y$ range up to 65.

Our least-squares experiment of Sec. IV C shows that all of the phenomenological formulas used in these experiments are not trustworthy in this range of $y$ values. Furthermore, our "data" are good to (at least) six decimal places, we have no problems of resolution[45] or inelasticity corrections,[46] and *still* these approximates are unable to extract the exponent $\eta$. Also the value $\frac{1}{4}$ is a large number for $\eta$,[47] and thus the two-dimensional Ising model should provide the *easiest* test for these phenomenological formulas. Thus we must conclude that any analysis of critical scattering data that makes use of the Fisher, Fisher-Burford, or $y^{-2+\eta}$ approximate must be seriously questioned when it comes to extracting the exponent $\eta$ from the scattering data.

We would like to give a series of steps that we feel will lead to an unambiguous measurement of $\eta$ (this assumes, of course, that the resolution and inelasticity corrections are also made). We consider the case $T > T_c$, and only at the end remark about the case $T < T_c$.

(i) Data must exist in both the large- and small-$k\xi$ regions (*a priori* one doesn't know large $k\xi$ from small $k\xi$, but in practice, some estimate for $\xi$ is usually available). The data in the small-$k\xi$ region in conjunction with the Ornstein-Zernike pole approximation allows one to determine $\xi$, and hence the scale variable $y = k\xi$. If the data are exceptionally good in the small $k\xi$ regime one might use a truncated version of (2.14) instead of the Ornstein-Zernike pole approximate.

(ii) Test the data to determine if it scales.

(iii) Determine the value of $y$ at which deviations from the Ornstein-Zernike pole first become significant (we denote this value by $y_{0Z}$).

(iv) For the data which satisfy $y > y_{0Z}$ (and $y \gg 1$) use the Fisher-Langer approximate (3.9) as a fitting function. To not have too many fitting parameters one might first set $C_3^* = 0$. As a check on the Fisher-Langer approximate, the value of the exponent $\alpha$ obtained from the least-squares fit should be compared with independent measurements of $\alpha$.

(v) If the data are good enough to have seen the exponent $\alpha$, then fixing $\alpha$ to the best known value is perhaps wise. A final fit with the Fisher-Langer approximate with this fixed $\alpha$ then gives an improved estimate for $\eta$. Furthermore if the data warrant it, one can include the $C_3^* y^{-1/\nu}$ term to get a better fit. This term may prove important for small $\alpha$.

(vi) The value of $\eta$ obtained should be independent of the cutoff $y_{0Z}$.

(vii) If data exist below $T_c$, then this can provide additional checks on the Fisher-Langer approximate. For instance, the only difference in the second term in (3.9) for above and below $T_c$ is the sign.

## ACKNOWLEDGMENTS

The authors wish to thank Professor T. T. Wu for many fruitful discussions and Professor C. N. Yang for much needed encouragement. We also wish to acknowledge useful discussions with Professor M. E. Fisher and Dr. B. Mozer. One of us (C.T.) would like to thank Professor E. W. Montroll for his interest and financial support, and Professor M. Blume for his hospitality extended at Brookhaven National Laboratory.

## APPENDIX A: SCALE VARIABLES AND SCALE FUNCTIONS $X_\pm(y)$

The two-dimensional Ising model on a square lattice is specified by the energy of interaction

$$\mathcal{E} = -E_1 \sum_{j,k} \sigma_{j,k}\sigma_{j,k+1} - E_2 \sum_{j,k} \sigma_{j,k}\sigma_{j+1,k}\,, \qquad \text{(A1)}$$

where the first (second) index of $\sigma_{j,k}$ specifies the row (column) of the lattice, and $\sigma_{j,k} = \pm 1$. In what follows we restrict ourselves to positive $E_1$ and $E_2$ (the ferromagnetic case).

It is useful to introduce the following notation: If an equation number is followed by an S, such as (A2S), that equation applies only to the symmetrical case $E_1 = E_2 = E$.

We define

$$z_1 = \tanh\beta E_1\,, \quad z_2 = \tanh\beta E_2\,, \qquad \text{(A2)}$$

and for the symmetrical lattice

$$z = z_1 = z_2 = \tanh\beta E\,, \qquad \text{(A2S)}$$

where $\beta = (k_B T)^{-1}$. At $T = T_c$

$$\sinh 2\beta_c E_1 \sinh 2\beta_c E_2 = 1\,, \qquad \text{(A3)}$$

or equivalently

$$z_{1c}z_{2c}+z_{1c}+z_{2c}-1=0\ . \tag{A4}$$

In particular, for the symmetric lattice,

$$z_c=\sqrt{2}-1\ . \tag{A4S}$$

In the limit $T\to T_c^{\pm}$, $M^2+N^2\to\infty$, such that $(T-T_c)\times(M^2+N^2)^{1/2}$ is fixed, then the spin-spin correlation function $\langle\sigma_{0,0}\sigma_{M,N}\rangle$ has been shown[11-13] to be of the scaling form

$$\langle\sigma_{0,0}\sigma_{M,N}\rangle=R^{-1/4}F_{\pm}(t)+O(R^{-5/4})\ , \tag{A5}$$

with

$$t=|z_1z_2+z_1+z_2-1|\left(\frac{M^2}{z_2(1-z_1^2)}+\frac{N^2}{z_1(1-z_2^2)}\right)^{1/2}$$
$$=|z_1z_2+z_1+z_2-1|\,[z_1z_2(1-z_1^2)(1-z_2^2)]^{-1/4}R\ , \tag{A6}$$

where

$$R=\left[\left(\frac{z_1(1-z_2^2)}{z_2(1-z_1^2)}\right)^{1/2}M^2+\left(\frac{z_2(1-z_1^2)}{z_1(1-z_2^2)}\right)^{1/2}N^2\right]^{1/2}$$
$$=\left[\left(\frac{\sinh2\beta E_1}{\sinh2\beta E_2}\right)^{1/2}M^2+\left(\frac{\sinh2\beta E_2}{\sinh2\beta E_1}\right)^{1/2}N^2\right]^{1/2}\ . \tag{A7}$$

If we define

$$\xi_{y,c}=|z_1z_2+z_1+z_2-1|^{-1}[z_2(1-z_1^2)]^{1/2} \tag{A8}$$

and

$$\xi_{x,c}=|z_1z_2+z_1+z_2-1|^{-1}[z_1(1-z_2^2)]^{1/2}\ , \tag{A9}$$

it follows from the work of Cheng and Wu[28] that if $\xi_x$ and $\xi_y$ denote the exact correlation lengths (above $T_c$), then

$$\lim_{T\to T_c}\left(\frac{\xi_x}{\xi_{x,c}}\right)=1\ ,\quad \lim_{T\to T_c}\left(\frac{\xi_y}{\xi_{y,c}}\right)=1\ . \tag{A10}$$

Thus in the critical region we can write $\xi_x\sim\xi_{x,c}$ and $\xi_y\sim\xi_{y,c}$. The subscript $c$ is to remind the reader that (A8) and (A9) are not the exact correlation lengths for all temperatures, but that (A8) and (A9) are asymptotically equal to the exact correlation lengths for $T\to T_c$. Thus (A6) and (A7) can be written as

$$t=\left[\left(\frac{M}{\xi_{y,c}}\right)^2+\left(\frac{N}{\xi_{x,c}}\right)^2\right]^{1/2}$$
$$=R/(\xi_{x,c}\,\xi_{y,c})^{1/2} \tag{A11}$$

and

$$R=\left[\left(\frac{\xi_{x,c}}{\xi_{y,c}}\right)^2M^2+\left(\frac{\xi_{y,c}}{\xi_{x,c}}\right)^2N^2\right]^{1/2}\ . \tag{A12}$$

For the symmetrical lattice we have

$$\xi_c\equiv\xi_{x,c}=\xi_{y,c}\ , \tag{A13S}$$

$$t=R/\xi_c\ , \tag{A11S}$$

and

$$R=(M^2+N^2)^{1/2}\ . \tag{A12S}$$

The $k$-dependent susceptibility $\chi(\vec{k},t)$ is by definition

$$\beta^{-1}\chi(\vec{k},T)=\sum_{M=-\infty}^{+\infty}\sum_{N=-\infty}^{+\infty}e^{i(k_xN+k_yM)}(\langle\sigma_{0,0}\sigma_{M,N}\rangle-\mathfrak{M}_s^2)\ , \tag{A14}$$

where $\mathfrak{M}_s$ is the spontaneous magnetization. If we are interested in the leading divergence of (A14) as $T\to T_c$, then as argued in Sec. VII A of Ref. 13 we can replace the discrete summation in (A14) by integrals to obtain for $T\to T_c^+$

$$\beta^{-1}\chi(\vec{k},T)\sim(\xi_{x,c}\,\xi_{y,c})\int_0^{\infty}t\,dt\int_{-\pi}^{\pi}d\phi\,\frac{F_+(t)}{R^{1/4}}$$
$$\times\exp(ik_x\,\xi_{x,c}\,t\cos\phi+ik_y\,\xi_{y,c}\,t\sin\phi)\ , \tag{A15}$$

where we used (A5). The only difference between (A15) and the case considered in Ref. 13 is the additional exponential factor in (A15). Performing the $\phi$ integration (A15) becomes

$$\beta^{-1}\chi(\vec{k},T)=2\pi(\xi_{x,c}\,\xi_{y,c})^{7/8}\int_0^{\infty}dt\,t^{3/4}F_+(t)\,J_0(ty)$$
$$+o((\xi_{x,c}\,\xi_{y,c})^{7/8})\ , \tag{A16}$$

with

$$y=(k_x^2\,\xi_{x,c}^2+k_y^2\,\xi_{y,c}^2)^{1/2}\ , \tag{A17}$$

which for the symmetrical lattice reduces to

$$\beta^{-1}\chi(\vec{k},T)=2\pi\,\xi_c^{7/4}\int_0^{\infty}dt\,t^{3/4}F_+(t)\,J_0(ty)+o(\xi_c^{7/4}) \tag{A16S}$$

and

$$y=k\xi_c\ ,\quad k=(k_x^2+k_y^2)^{1/2}\ . \tag{A17S}$$

The case below $T_c$ is similar and we obtain

$$\beta^{-1}\chi(\vec{k},T)=2\pi(\xi_{x,c}\,\xi_{y,c})^{7/8}\int_0^{\infty}dt[t^{3/4}F_-(t)$$
$$-(\sinh2\beta_cE_1+\sinh2\beta_cE_2)^{1/8}2^{1/4}t]\,J_0(ty)$$
$$+o((\xi_{x,c}\,\xi_{y,c})^{7/8})\ , \tag{A18}$$

which for the symmetric lattice reduces to

$$\beta^{-1}\chi(\vec{k},T)=2\pi\xi_c^{7/4}$$
$$\times\int_0^{\infty}dt[t^{3/4}F_-(t)-2^{3/8}t]\,J_0(ty)+o(\xi^{7/4})\ . \tag{A18S}$$

Thus the scale functions $X_{\pm}(y)$ are given by

$$X_+(y)=2\pi\int_0^{\infty}dt\,t^{3/4}F_+(t)\,J_0(ty) \tag{A19}$$

and

$$X_-(y)=2\pi\int_0^{\infty}dt[t^{3/4}F_-(t)-2^{1/4}(\sinh2\beta_cE_1$$
$$+\sinh2\beta_cE_2)^{1/8}t]\,J_0(ty)\ , \tag{A20}$$

with $y$ given by (A17) [and (A17S) for the symmetric

lattice], and $J_0(x)$ is the zeroth-order Bessel function. Using the fact that $|J_0(x)| \le 1$ for real $x$ and the fact that the factors multiplying $J_0(ty)$ in (A19) and (A20) are non-negative, we obtain

$$X_\pm(y) \le X_\pm(0) \quad \text{for all real } y\ . \tag{A21}$$

## APPENDIX B: $X_\pm(y)$ IN TERMS OF A PAINLEVÉ FUNCTION

The scale functions $F_\pm(t)$ of (A5) may be expressed in terms of a Painlevé function (of third kind) which we call $\eta(\theta)$.[11-13] This Painlevé function satisfies the second-order nonlinear differential equation

$$\frac{d^2\eta(\theta)}{d\theta^2} = \frac{1}{\eta(\theta)}\left(\frac{d\eta(\theta)}{d\theta}\right)^2 - \eta^{-1}(\theta) + \eta^3(\theta) - \frac{1}{\theta}\left(\frac{d\eta(\theta)}{d\theta}\right), \tag{B1}$$

with the boundary conditions

$$\eta(\theta) = -\theta[\ln(\theta/4) + \gamma_E] + O(\theta^5 \ln^3\theta) \tag{B2}$$

as $\theta \to 0$, $\gamma_E = 0.577\,215\,665\ldots$ is Euler's constant, and

$$\eta(\theta) = 1 - 2\pi^{-1}K_0(2\theta) + O(e^{-4\theta}) \tag{B3}$$

as $\theta \to \infty$, where $K_0(x)$ is the zeroth-order Bessel function of third kind. We then have[11-13]

$$F_\pm(t) = 2^{-1/2}(\sinh 2\beta_c E_1 + \sinh 2\beta_c E_2)^{1/8}\theta^{1/4}[1 \mp \eta(\theta)] \times \exp\left(\int_\theta^\infty dx\, x \ln x[1 - \eta^2(x)] - h(\theta)\right), \tag{B4}$$

where

$$\theta = \tfrac{1}{2}t \tag{B5}$$

and

$$h(\theta) = \left(\frac{\theta\eta'}{2\eta} + \frac{\theta^2}{4\eta^2}[(1-\eta^2)^2 - \eta'^2]\right)\ln\theta\ . \tag{B6}$$

Then using (B4) in (A19) and (A20) we obtain

$$X_+(y) = 2^{9/4}\pi(\sinh 2\beta_c E_1 + \sinh 2\beta_c E_2)^{1/8}\int_0^\infty d\theta\,\theta[1-\eta(\theta)]\exp\left(\int_\theta^\infty dx\, x\ln x[1-\eta^2(x)] - h(\theta)\right)J_0(2\theta y) \tag{B7}$$

and

$$X_-(y) = 2^{9/4}\pi(\sinh 2\beta_c E_1 + \sinh 2\beta_c E_2)^{1/8}\int_0^\infty d\theta\,\theta\left[[1+\eta(\theta)]\exp\left(\int_\theta^\infty dx\, x\ln x[1-\eta^2(x)] - h(\theta)\right) - 2\right]J_0(2\theta y)\ , \tag{B8}$$

respectively. Equations (B7) and (B8) are exact. From a numerical standpoint (B7) and (B8) are most useful as we only need to solve (B1) numerically [subject to the boundary conditions (B2) and (B3)] and then perform two integrations (again numerically) to obtain $X_\pm(y)$. In Table VIII we give the numerical values of $X_\pm(y)/X_\pm(0)$ for $0 \le y \le 20$. For $y > 20$ the expansion (2.10) may be used to compute $X_\pm(y)$.

## APPENDIX C: DISPERSION REPRESENTATION FOR $X_\pm(y)$

In Ref. 13 it was found useful to write $F_\pm(t)$ [see (A5)] as

$$F_\pm(t) = (2t)^{1/4}(\sinh 2\beta_c E_1 + \sinh 2\beta_c E_2)^{1/8}\hat{F}_\pm(t)\ , \tag{C1}$$

so that (A19) and (A20) become

$$X_+(y) = 2\pi 2^{1/4}(\sinh 2\beta_c E_1 + \sinh 2\beta_c E_2)^{1/8} \times \int_0^\infty dt\, t\hat{F}_+(t)J_0(ty) \tag{C2}$$

and

$$X_-(y) = 2\pi 2^{1/4}(\sinh 2\beta_c E_1 + \sinh 2\beta_c E_2)^{1/8} \times \int_0^\infty dt\, t[\hat{F}_-(t) - 1]J_0(ty)\ , \tag{C3}$$

respectively. It was found[13] that $\hat{F}_\pm(t)$ could be written as

$$\hat{F}_-(t) = \exp\left(-\sum_{n=1}^\infty f^{(2n)}(t)\right), \tag{C4}$$

$$\hat{F}_+(t) = G(t)\hat{F}_-(t)\ , \tag{C5}$$

$$G(t) = \sum_{k=0}^\infty g^{(2k+1)}(t)\ , \tag{C6}$$

with

$$f^{(2n)}(t) = (-1)^n\pi^{-2n}n^{-1}\int_1^\infty dy_1 \cdots \int_1^\infty dy_{2n} \times \prod_{j=1}^{2n}\frac{e^{-ty_j}}{(y_j^2-1)^{1/2}(y_j+y_{j+1})}\prod_{j=1}^{n}(y_{2j}^2-1) \tag{C7}$$

($y_{2n+1} \equiv y_1$) and

$$g^{(2k+1)}(t) = (-1)^k\pi^{-(2k+1)}\int_1^\infty dy_1 \cdots \int_1^\infty dy_{2k+1} \times \prod_{j=1}^{2k+1}\frac{e^{-tj}}{(y_j^2-1)^{1/2}}\prod_{j=1}^{2k}(y_j+y_{j+1})^{-1}\prod_{j=1}^{k}(y_{2j}^2-1) \tag{C8}$$

(for $k = 0$ the last two products are replaced by unity). For $t \to \infty$, $f^{(2n)}(t)$ and $g^{(2k+1)}(t)$ behave as

TABLE VIII. Scale functions $X_{\pm}(y)/X_{\pm}(0)$ for two-dimensional Ising model for the range $0 \le y \le 20$. The values of $X_{\pm}(0)$ for the symmetric lattice are given in Table II.

| $y$ | $X_+(y)/X_+(0)$ | $X_-(y)/X_-(0)$ | $y$ | $X_+(y)/X_+(0)$ | $X_-(y)/X_-(0)$ |
|---|---|---|---|---|---|
| 0.0 | 1.0 | 1.0 | 9.6 | $0.111\,969\times10^{-1}$ | 0.172 715 |
| 0.1 | 0.990 107 06 | 0.999 002 56 | 9.8 | $0.107\,619\times10^{-1}$ | 0.168 097 |
| 0.2 | 0.961 569 44 | 0.996 026 65 | 10.0 | $0.103\,523\times10^{-1}$ | 0.163 670 |
| 0.3 | 0.917 497 53 | 0.991 122 56 | 10.2 | $0.996\,593\times10^{-2}$ | 0.159 421 |
| 0.4 | 0.862 179 65 | 0.984 371 14 | 10.4 | $0.960\,117\times10^{-2}$ | 0.155 343 |
| 0.5 | 0.800 160 26 | 0.975 880 17 | 10.6 | $0.925\,644\times10^{-2}$ | 0.151 425 |
| 0.6 | 0.735 505 89 | 0.965 779 53 | 10.8 | $0.893\,024\times10^{-2}$ | 0.147 660 |
| 0.7 | 0.671 403 59 | 0.954 215 94 | 11.0 | $0.862\,129\times10^{-2}$ | 0.144 039 |
| 0.8 | 0.610 067 15 | 0.941 347 30 | 11.2 | $0.832\,836\times10^{-2}$ | 0.140 555 |
| 0.9 | 0.552 842 10 | 0.927 337 32 | 11.4 | $0.805\,043\times10^{-2}$ | 0.137 202 |
| 1.0 | 0.500 396 69 | 0.912 350 74 | 11.6 | $0.778\,644\times10^{-2}$ | 0.133 973 |
| 1.2 | 0.410 302 | 0.880 086 | 11.8 | $0.753\,544\times10^{-2}$ | 0.130 861 |
| 1.4 | 0.338 357 | 0.845 751 | 12.0 | $0.729\,662\times10^{-2}$ | 0.127 861 |
| 1.6 | 0.281 458 | 0.810 373 | 12.2 | $0.706\,917\times10^{-2}$ | 0.124 967 |
| 1.8 | 0.236 439 | 0.774 775 | 12.4 | $0.685\,245\times10^{-2}$ | 0.122 175 |
| 2.0 | 0.200 612 | 0.739 595 | 12.6 | $0.664\,577\times10^{-2}$ | 0.119 480 |
| 2.2 | 0.171 861 | 0.705 292 | 12.8 | $0.644\,845\times10^{-2}$ | 0.116 877 |
| 2.4 | 0.148 569 | 0.672 180 | 13.0 | $0.625\,997\times10^{-2}$ | 0.114 362 |
| 2.6 | 0.129 513 | 0.640 468 | 13.2 | $0.607\,982\times10^{-2}$ | 0.111 931 |
| 2.8 | 0.113 774 | 0.610 265 | 13.4 | $0.590\,751\times10^{-2}$ | 0.109 581 |
| 3.0 | 0.100 654 | 0.581 622 | 13.6 | $0.574\,258\times10^{-2}$ | 0.107 307 |
| 3.2 | $0.896\,222\times10^{-1}$ | 0.554 543 | 13.8 | $0.558\,460\times10^{-2}$ | 0.105 106 |
| 3.4 | $0.802\,707\times10^{-1}$ | 0.529 002 | 14.0 | $0.543\,321\times10^{-2}$ | 0.102 976 |
| 3.6 | $0.722\,838\times10^{-1}$ | 0.504 942 | 14.2 | $0.528\,803\times10^{-2}$ | 0.100 913 |
| 3.8 | $0.654\,139\times10^{-1}$ | 0.482 305 | 14.4 | $0.514\,872\times10^{-2}$ | $0.989\,136\times10^{-1}$ |
| 4.0 | $0.594\,664\times10^{-1}$ | 0.461 017 | 14.6 | $0.501\,497\times10^{-2}$ | $0.969\,762\times10^{-1}$ |
| 4.2 | $0.542\,860\times10^{-1}$ | 0.440 999 | 14.8 | $0.488\,649\times10^{-2}$ | $0.950\,979\times10^{-1}$ |
| 4.4 | $0.497\,485\times10^{-1}$ | 0.422 176 | 15.0 | $0.476\,300\times10^{-2}$ | $0.932\,765\times10^{-1}$ |
| 4.6 | $0.457\,531\times10^{-1}$ | 0.404 475 | 15.2 | $0.464\,424\times10^{-2}$ | $0.915\,092\times10^{-1}$ |
| 4.8 | $0.422\,180\times10^{-1}$ | 0.387 820 | 15.4 | $0.452\,998\times10^{-2}$ | $0.897\,941\times10^{-1}$ |
| 5.0 | $0.390\,758\times10^{-1}$ | 0.372 140 | 15.6 | $0.441\,998\times10^{-2}$ | $0.881\,293\times10^{-1}$ |
| 5.2 | $0.362\,710\times10^{-1}$ | 0.357 374 | 15.8 | $0.431\,404\times10^{-2}$ | $0.865\,123\times10^{-1}$ |
| 5.4 | $0.337\,574\times10^{-1}$ | 0.343 453 | 16.0 | $0.421\,196\times10^{-2}$ | $0.849\,417\times10^{-1}$ |
| 5.6 | $0.314\,964\times10^{-1}$ | 0.330 321 | 16.2 | $0.411\,355\times10^{-2}$ | $0.834\,156\times10^{-1}$ |
| 5.8 | $0.294\,555\times10^{-1}$ | 0.317 926 | 16.4 | $0.401\,863\times10^{-2}$ | $0.819\,323\times10^{-1}$ |
| 6.0 | $0.276\,072\times10^{-1}$ | 0.306 214 | 16.6 | $0.392\,704\times10^{-2}$ | $0.804\,900\times10^{-1}$ |
| 6.2 | $0.259\,281\times10^{-1}$ | 0.295 141 | 16.8 | $0.383\,864\times10^{-2}$ | $0.790\,874\times10^{-1}$ |
| 6.4 | $0.243\,984\times10^{-1}$ | 0.284 663 | 17.0 | $0.375\,325\times10^{-2}$ | $0.777\,229\times10^{-1}$ |
| 6.6 | $0.230\,008\times10^{-1}$ | 0.274 740 | 17.2 | $0.367\,076\times10^{-2}$ | $0.763\,953\times10^{-1}$ |
| 6.8 | $0.217\,207\times10^{-1}$ | 0.265 334 | 17.4 | $0.359\,104\times10^{-2}$ | $0.751\,030\times10^{-1}$ |
| 7.0 | $0.205\,454\times10^{-1}$ | 0.256 410 | 17.6 | $0.351\,394\times10^{-2}$ | $0.738\,448\times10^{-1}$ |
| 7.2 | $0.194\,636\times10^{-1}$ | 0.247 938 | 17.8 | $0.343\,937\times10^{-2}$ | $0.726\,197\times10^{-1}$ |
| 7.4 | $0.184\,657\times10^{-1}$ | 0.239 888 | 18.0 | $0.336\,721\times10^{-2}$ | $0.714\,260\times10^{-1}$ |
| 7.6 | $0.175\,434\times10^{-1}$ | 0.232 233 | 18.2 | $0.329\,736\times10^{-2}$ | $0.702\,634\times10^{-1}$ |
| 7.8 | $0.166\,891\times10^{-1}$ | 0.224 948 | 18.4 | $0.322\,972\times10^{-2}$ | $0.691\,301\times10^{-1}$ |
| 8.0 | $0.158\,964\times10^{-1}$ | 0.218 010 | 18.6 | $0.316\,420\times10^{-2}$ | $0.680\,252\times10^{-1}$ |
| 8.2 | $0.151\,595\times10^{-1}$ | 0.211 397 | 18.8 | $0.310\,071\times10^{-2}$ | $0.669\,483\times10^{-1}$ |
| 8.4 | $0.144\,733\times10^{-1}$ | 0.205 090 | 19.0 | $0.303\,915\times10^{-2}$ | $0.658\,978\times10^{-1}$ |
| 8.6 | $0.138\,332\times10^{-1}$ | 0.199 069 | 19.2 | $0.297\,946\times10^{-2}$ | $0.648\,732\times10^{-1}$ |
| 8.8 | $0.132\,351\times10^{-1}$ | 0.193 319 | 19.4 | $0.292\,157\times10^{-2}$ | $0.638\,733\times10^{-1}$ |
| 9.0 | $0.126\,755\times10^{-1}$ | 0.187 823 | 19.6 | $0.286\,540\times10^{-2}$ | $0.628\,977\times10^{-1}$ |
| 9.2 | $0.121\,511\times10^{-1}$ | 0.182 566 | 19.8 | $0.281\,087\times10^{-2}$ | $0.619\,454\times10^{-1}$ |
| 9.4 | $0.116\,591\times10^{-1}$ | 0.177 534 | | | |

$$f^{(2n)}(t) = (-1)^n \pi^{-n} (2n)^{-1} 2^{-3n+1} \frac{e^{-2nt}}{t^{2n}} \left(1 - \tfrac{7}{4} n t^{-1} + O(t^{-2})\right) \tag{C9}$$

and

$$g^{(2k+1)}(t) = (-1)^k \pi^{-k-1/2} 2^{-3k-1/2} \times \frac{e^{-(2k+1)t}}{t^{2k+1/2}} \left[1 - \tfrac{1}{8}(14k+1) t^{-1} + O(t^{-2})\right], \tag{C10}$$

respectively. Expanding the exponential in (C4) we can write (C4) and (C5) as

$$\hat{F}_-(t) = 1 + \sum_{n=1}^{\infty} \hat{F}_-^{(2n)}(t) , \tag{C11}$$

with

$$\hat{F}_-^{(2)}(t) = -f^{(2)}(t) , \tag{C12a}$$

$$\hat{F}_-^{(4)}(t) = -f^{(4)}(t) + (1/2!)[f^{(2)}(t)]^2 , \tag{C12b}$$

$$\hat{F}_-^{(6)}(t) = -f^{(6)}(t) + f^{(2)}(t)f^{(4)}(t) - (1/3!)[f^{(2)}(t)]^3 , \tag{C12c}$$

etc., and

$$\hat{F}_+(t) = \sum_{k=0}^{\infty} \hat{F}_+^{(2k+1)}(t) , \tag{C13}$$

with

$$\hat{F}_+^{(1)}(t) = g^{(1)}(t) , \tag{C14a}$$

$$\hat{F}_+^{(3)}(t) = g^{(3)}(t) + g^{(1)}(t)\hat{F}_-^{(2)}(t) = g^{(3)}(t) - g^{(1)}(t)f^{(2)}(t) , \tag{C14b}$$

$$\hat{F}_+^{(5)}(t) = g^{(5)}(t) + g^{(3)}(t)\hat{F}_-^{(2)}(t) + g^{(1)}(t)\hat{F}_-^{(4)}(t) = g^{(5)}(t) - g^{(3)}(t)f^{(2)}(t) + g^{(1)}(t) \times \{-f^{(4)}(t) + \tfrac{1}{2}[f^{(2)}(t)]^2\} , \tag{C14c}$$

etc., respectively. From (C1), (C11), and (C12) we see that $F_-^{(2n)}(t)$ behaves as $e^{-2nt}$ as $t \to \infty$; similarly from (C9), (C10), (C13), and (C14) it follows that $\hat{F}_+^{(2k+1)}(t)$ behaves as $e^{-(2k+1)t}$ as $t \to \infty$. Here the term "behaves as $e^{-at}$" means that as $t \to \infty$ the quantity is asymptotically equal to $e^{-at}$ times some power at $t$.

Using (C11) in (C3) and (C13) in (C2) we obtain

$$X_+(y) = \sum_{n=1}^{\infty} X_+^{(2n-1)}(y) \tag{C15}$$

and

$$X_-(y) = \sum_{n=1}^{\infty} X_-^{(2n)}(y) , \tag{C16}$$

where

$$X_+^{(2n-1)}(y) = 2\pi 2^{1/4}(\sinh 2\beta_c E_1 + \sinh 2\beta_c E_2)^{1/8} \times \int_0^{\infty} dt\, t\hat{F}_+^{(2n-1)}(t) J_0(ty) \tag{C17}$$

and

$$X_-^{(2n)}(y) = 2\pi 2^{1/4}(\sinh 2\beta_c E_1 + \sinh 2\beta_c E_2)^{1/8} \times \int_0^{\infty} dt\, t\hat{F}_-^{(2n)}(t) J_0(ty) . \tag{C18}$$

From the large-$t$ behavior of $\hat{F}_+^{(2n-1)}(t)$ [$\hat{F}_-^{(2n)}(t)$] it follows that $X_+^{(2n-1)}(y)$ [$X_-^{(2n-1)}(y)$] has singularities at $y = \pm(2n-1)i$ [$\pm 2ni$]. Thus from (C15) [(C16)] we see that $X_+(y)$ [$X_-(y)$] has singularities at $\pm(2n-1)i$ [$\pm 2ni$] for $n = 1, 2, 3, \ldots$.

From Ref. 13 we have

$$\hat{F}_+^{(1)}(t) = \pi^{-1}K_0(t) , \tag{C19}$$

where $K_0(t)$ is the modified Bessel function. Substituting (C19) into (C17) (for $n=1$) we obtain

$$X_+^{(1)}(y) = 2^{5/4}(\sinh 2\beta_c E_1 + \sinh 2\beta_c E_2)^{1/8}(1+y^2)^{-1} . \tag{C20}$$

This is the Ornstein-Zernike pole term.

Also from Ref. 13 we have

$$\hat{F}_-^{(2)}(t) = \pi^{-2}\{t^2[K_1^2(t) - K_0^2(t)] - tK_1(t)K_0(t) + \tfrac{1}{2}K_0^2(t)\} . \tag{C21}$$

Using (C21) in (C18) [for $n=1$] we have

$$X_-^{(2)}(y) = 2^{5/4}(\sinh 2\beta_c E_1 + \sinh 2\beta_c E_2)^{1/8}\pi^{-1}\left(\int_0^{\infty} dt\, t^3[K_1^2(t) - K_0^2(t)]J_0(ty) - \int_0^{\infty} dt\, t^2 K_1(t)K_0(t)J_0(ty) + \frac{1}{2}\int_0^{\infty} dt\, tK_0^2(t)J_0(yt)\right) . \tag{C22}$$

To put the integrals occurring in (C22) into a standard form we first use Nicholson's formula[48]

$$K_\mu(z)K_\nu(z) = 2\int_0^{\infty} K_{\mu\pm\nu}(2z\cosh s)\cosh(\mu \pm \nu)s\, ds \tag{C23}$$

in (C22) to obtain

$$X_-^{(2)}(y) = 2^{5/4}(\sinh 2\beta_c E_1 + \sinh 2\beta_c E_2)^{1/8}\pi^{-1}\left(\frac{1}{2}\int_0^{\infty} ds \frac{\cosh 2s}{\cosh^4 s} F(2, 2; 1; -\lambda) - \frac{1}{2}\int_0^{\infty} \frac{ds}{\cosh^4 s} F(2, 2; 1; -\lambda) - \frac{1}{2}\int_0^{\infty} \frac{ds}{\cosh^2 s} F(2, 1; 1; -\lambda) + \frac{1}{4}\int_0^{\infty} \frac{ds}{\cosh^2 s} F(1, 1; 1; -\lambda)\right) , \tag{C24}$$

where $\lambda = y^2(4\cosh^2 s)^{-1}$, $F(a, b; c; z)$ is the hypergeometric function of Gauss,[49] and where we used[50]

$$\int_0^{\infty} dx\, x^{\lambda}K_\mu(ax)J_0(bx) = 2^{\lambda-1}\Gamma\left(\frac{\lambda+\mu+1}{2}\right)\Gamma\left(\frac{\lambda-\mu+1}{2}\right)a^{-\lambda-1}F\left(\frac{\lambda+\mu+1}{2}, \frac{\lambda-\mu+1}{2}; 1; -\frac{b^2}{a^2}\right) . \tag{C25}$$

Letting $x = \cosh s$ in (C24) we obtain

$$X_-^{(2)}(y)=2^{5/4}(\sinh 2\beta_c E_1+\sinh 2\beta_c E_2)^{1/8}\pi^{-1}\int_1^\infty \frac{dx}{(x^2-1)^{1/2}}\left\{\left[\left(\frac{x^2-1}{x^4}\right)F\left(2,2;1;-\frac{y^2}{4x^2}\right)\right.\right.$$
$$\left.\left.-\frac{1}{2x^2}F\left(2,1;1;-\frac{y^2}{4x^2}\right)+\frac{1}{4x^2}F\left(1,1;1;-\frac{y^2}{4x^2}\right)\right]\right\}. \quad \text{(C26)}$$

The hypergeometric functions appearing in (C26) are elementary.[51] We have

$$F(1,1;1;z)=(1-z)^{-1},$$
$$F(1,2;1;z)=(1-z)^{-2},$$
and (C27)
$$F(2,2;1;z)=(1+z)(1-z)^{-3}.$$

Using (C27) in (C26)

$$X_-^{(2)}(y)=2^{5/4}(\sinh 2\beta_c E_1+\sinh 2\beta_c E_2)^{1/8}\pi^{-1}$$
$$\times\left[\tfrac{3}{4}I_2-(1+\tfrac{1}{4}y^2)I_1+(\tfrac{1}{4}y^2)(1+\tfrac{1}{16}y^2)I_0\right], \quad \text{(C28)}$$

with

$$I_n=\int_1^\infty \frac{dx}{(x^2-1)^{1/2}}\frac{x^{2n}}{(x^2+\frac{1}{4}y^2)^3}. \quad \text{(C29)}$$

The integral (C29) is of standard form[52] (let $x^2=u$) and we have

$$I_n=\tfrac{1}{2}B(3-n,\tfrac{1}{2})F(3,3-n;\tfrac{7}{2}-n;-\tfrac{1}{4}y^2), \quad \text{(C30)}$$

where $B(x,y)$ is the beta function. Finally one can show that[53,54]

$$F(3,1;\tfrac{3}{2};-z^2)=\frac{3\ln[z+(z^2+1)^{1/2}]}{8z(1+z^2)^{5/2}}+\frac{5+2z^2}{8(1+z^2)^2}, \quad \text{(C31a)}$$

$$F(3,2;\tfrac{5}{2};-z^2)=\frac{3(1+4z^2)\ln[z+(z^2+1)^{1/2}]}{16z^3(1+z^2)^{5/2}}$$
$$-\frac{3(1-2z^2)}{16z^2(1+z^2)^2}, \quad \text{(C31b)}$$

and

$$F(3,3;\tfrac{7}{2};-z^2)=\frac{15}{64}\frac{\ln[z+(z^2+1)^{1/2}]}{z^5(1+z^2)^{5/2}}(8z^4+8z^2+3)$$
$$-\frac{45}{64}\frac{(1+2z^2)}{z^4(1+z^2)^2}. \quad \text{(C31c)}$$

Using (C30) and (C31) in (C28) we obtain (upon simplification) (2.6). From (2.6) we can calculate (2.5). From (2.6) it is clear that $X_-^{(2)}(y)$ has square-root branch points at $y=\pm 2i$. There is no logarithmic branch point in $\rho_-^{(2)}(y)$ since the quantity $[z+(z^2+1)^{1/2}]$ does not vanish in the finite $z$ plane.

In general $X_-^{(2n)}(y)$ has square-root branch points at $y=2ni$. To see this we note that from (C12) and (C9) it follows that

$$\hat{F}_-^{(2n)}(t)\sim A_n e^{-2nt}/t^\lambda \quad (t\to\infty), \quad \text{(C32)}$$

where $\lambda$ is a positive integer greater than or equal to $2n$, and $A_n$ is a constant. For $n=1$, $\lambda=2$, and for $n=2$, $\lambda=8$. Then using (C32) in (C18) we conclude that

$$X_-^{(2n)}(iy)\sim 2^{1/4}(\sinh 2\beta_c E_1+\sinh 2\beta_c E_2)^{1/8}$$
$$\times A_n(\pi/n)^{1/2}\Gamma(\tfrac{3}{2}-\lambda)(2n-y)^{\lambda-3/2} \quad \text{(C33)}$$

for $y\to 2n^-$. Thus the singularity at $y=+2ni$ is a square-root branch point. Since $X_-^{(2n)}(y)$ is even the same type of singularity occurs at $y=-2ni$. A similar argument shows that the singularities of $X_+^{(2n+1)}(y)$ at $y=\pm(2n+1)i$ are square-root branch points.

In Ref. 13 it is shown that we can write

$$\hat{F}_+^{(2n-1)}(t)=\int_1^\infty dy_1\cdots\int_1^\infty dy_{2n-1}$$
$$\times e^{-t(y_1+\cdots+y_{2n-1})}\mathfrak{F}_+^{(2n-1)}(y_1,y_2,\ldots,y_{2n-1}) \quad \text{(C34)}$$

and

$$\hat{F}_-^{(2n)}(t)=\int_1^\infty dy_1\cdots\int_1^\infty dy_{2n}$$
$$\times e^{-t(y_1+\cdots+y_{2n})}\mathfrak{F}_-^{(2n)}(y_1,y_2,\ldots,y_{2n}), \quad \text{(C35)}$$

where $\mathfrak{F}_\pm$ are functions of $y_j$ but not $t$. In particular, from Ref. 13 [or using (C7) and (C8) in (C12) and (C14)] we know that

$$\mathfrak{F}_+^{(1)}(y_1)=\pi^{-1}(y_1^2-1)^{-1/2}, \quad \text{(C36a)}$$

$$\mathfrak{F}_+^{(3)}(y_1,y_2,y_3)=2^{-1}\pi^{-3}\left(\frac{y_2^2-1}{(y_1^2-1)(y_3^2-1)}\right)^{1/2}$$
$$\times\left(\frac{y_1-y_3}{(y_1+y_2)(y_2+y_3)}\right)^2, \quad \text{(C36b)}$$

and

$$\mathfrak{F}_-^{(2)}(y_1,y_2)=\pi^{-2}\left(\frac{y_2^2-1}{y_4^2-1}\right)^{1/2}(y_1+y_2)^{-2}, \quad \text{(C37a)}$$

$$\mathfrak{F}_-^{(4)}(y_1,y_2,y_3,y_4)=4^{-1}\pi^{-4}\left(\frac{(y_2^2-1)(y_4^2-1)}{(y_1^2-1)(y_3^2-1)}\right)^{1/2}$$
$$\times\left(\frac{(y_2-y_4)(y_1-y_3)}{(y_1+y_2)(y_2+y_3)(y_3+y_4)(y_4+y_1)}\right)^2, \quad \text{(C37b)}$$

etc. One can easily write expressions for the next few $\mathfrak{F}_+^{(2n-1)}$ and $\mathfrak{F}_-^{(2n)}$ by using (C7) and (C8) in (C12) and (C14). Note that (C36b) and (C37b) are not just simply what one obtains by substituting (C7) and (C8) into (C12) and (C14). Certain other simplifications have been made (see Ref. 13).

Given (C34) and (C35) we see that

$$X_+^{(2n-1)}(y)=2\pi 2^{1/4}(\sinh 2\beta_c E_1+\sinh 2\beta_c E_2)^{1/8}$$

$$\times\int_1^\infty dy\cdots\int_1^\infty dy_{2n-1}\mathcal{F}_+^{(2n-1)}(y_1,\ldots,y_{2n-1})$$

$$\times\frac{y_1+y_2+\cdots+y_{2n-1}}{[(y_1+y_2+\cdots+y_{2n-1})^2+y^2]^{3/2}} \tag{C38}$$

and

$$X_-^{(2n)}(y)=2\pi 2^{1/4}(\sinh 2\beta_c E_1+\sinh 2\beta_c E_2)^{1/8}$$

$$\times\int_1^\infty dy_1\cdots\int_1^\infty dy_{2n}\mathcal{F}_-^{(2n)}(y_1,\ldots,y_{2n})$$

$$\times\frac{y_1+y_2+\cdots+y_{2n}}{[(y_1+y_2+\cdots+y_{2n})^2+y^2]^{3/2}}\,, \tag{C39}$$

where we made use of the definite integral

$$\int_0^\infty dt\,t\,e^{-\alpha t}J_0(ty)=\alpha(\alpha^2+y^2)^{-3/2}\,. \tag{C40}$$

The square-root branch-point structure of $X_+^{(2n-1)}(y)$ $[X_-^{(2n)}(y)]$ is especially clear from (C38) [(C39)]. We can summarize the results we have so far obtained by (2.1)–(2.4).

In terms of $X_+^{(2n-1)}(y)$ and $X_-^{(2n)}(y)$ we can write the spectral functions $\rho_+^{(2n-1)}(y)$ and $\rho_-^{(2n)}(y)$ (for $y$ real) as

$$\rho_+^{(2n-1)}(y)=i\pi^{-1}y[X_+^{(2n-1)}(iy+0)-X_+^{(2n-1)}(iy-0)] \tag{C41}$$

and

$$\rho_-^{(2n)}(y)=i\pi^{-1}y[X_-^{(2n)}(iy+0)-X_-^{(2n)}(iy-0)]\,, \tag{C42}$$

where

$$X_\pm^{(n)}(iy\pm 0)\equiv\lim_{\epsilon\to 0}X_\pm^{(n)}(iy\pm\epsilon)\,,\quad \epsilon,\ y\ \text{real}\,. \tag{C43}$$

Numerically the integrals (C38) and (C39) can be evaluated for $n$ small by multiple Gaussian integration. This is how we obtained $X_+^{(3)}(0)$, $X_+^{(5)}(0)$, and $X_-^{(4)}(0)$ in Table II. A table of values of $X_+^{(3)}(y)/X_+^{(3)}(0)$ is given in Table IX.

TABLE IX. This table gives the three-particle contribution i.e., $X_+^{(3)}(y)$, to the scale function $X_+(y)$. At $y=0$, $X_+^{(3)}(0)=0.002\,112\,454\,5415\ldots$.

| $y$ | $X_+^{(3)}(y)/X_+^{(3)}(0)$ | $y$ | $X_+^{(3)}(y)/X_+^{(3)}(0)$ |
|---|---|---|---|
| 0.0 | 1.0 | 9.5 | 0.582 10 |
| 0.5 | 0.996 71 | 10.0 | 0.563 54 |
| 1.0 | 0.987 00 | 11.0 | 0.528 98 |
| 1.5 | 0.971 43 | 12.0 | 0.497 57 |
| 2.0 | 0.951 73 | 13.0 | 0.468 99 |
| 2.5 | 0.928 40 | 14.0 | 0.442 93 |
| 3.0 | 0.902 74 | 15.0 | 0.419 12 |
| 3.5 | 0.875 66 | 16.0 | 0.397 32 |
| 4.0 | 0.847 87 | 17.0 | 0.377 30 |
| 4.5 | 0.819 99 | 18.0 | 0.358 89 |
| 5.0 | 0.792 34 | 19.0 | 0.341 91 |
| 5.5 | 0.765 31 | 20.0 | 0.326 21 |
| 6.0 | 0.739 03 | 22.0 | 0.298 17 |
| 6.5 | 0.713 61 | 24.0 | 0.273 91 |
| 7.0 | 0.689 18 | 26.0 | 0.252 77 |
| 7.5 | 0.665 80 | 28.0 | 0.234 21 |
| 8.0 | 0.643 41 | 30.0 | 0.217 81 |
| 8.5 | 0.622 01 | 32.0 | 0.203 24 |
| 9.0 | 0.601 56 | 34.0 | 0.190 22 |
| | | 36.0 | 0.178 54 |
| | | 38.0 | 0.168 00 |
| | | 40.0 | 0.158 46 |

## APPENDIX D: LARGE-$y$ BEHAVIOR OF $X_\pm(y)$, $X_+^{(2n-1)}(y)$, AND $X_-^{(2n)}(y)$

The large-$y$ behavior of $X_\pm(y)$ is determined by the small-$t$ behavior of $F_\pm(t)$ [see (A19) and (A20)]. From Ref. 13 we have for $t\to 0$

$$F_\pm(t)=F(0)[1\pm\tfrac{1}{2}t\Omega+\tfrac{1}{16}t^2\pm\tfrac{1}{32}t^3\Omega$$

$$+\tfrac{1}{256}t^4(-\Omega^2+\Omega+\tfrac{1}{8})+O(t^5\Omega^4)]\,, \tag{D1}$$

with

$$\Omega=\ln(t/8)+\gamma_E\,, \tag{D2a}$$

$\gamma_E=$ Euler's constant,

$$F(0)=(\sinh 2\beta_c E_1+\sinh 2\beta_c E_2)^{1/8}e^{1/4}2^{1/12}A^{-3}\,, \tag{D2b}$$

and

$A=$ Glaisher's constant $=1.282\,427\,129\,100\,62\ldots$. (D2c)

Using (D1) in (A19) and (A20) we obtain (2.10), where

$$C_1=F(0)2^{7/4}[\Gamma(\tfrac{7}{8})]^2\cos\tfrac{3}{8}\pi\,, \tag{D3a}$$

$$C_2=\left(\frac{\Gamma(\frac{11}{8})}{\Gamma(\frac{7}{8})}\right)^2\tan\tfrac{3}{8}\pi\,, \tag{D3b}$$

$$C_3=-\tan\tfrac{3}{8}\pi\left(\frac{\Gamma(\frac{11}{8})}{\Gamma(\frac{7}{8})}\right)^2[\gamma_E-2\ln 2+\psi(\tfrac{11}{8})-\tfrac{1}{2}\pi\tan\tfrac{7}{8}\pi]\,, \tag{D3c}$$

$$C_4=-\tfrac{49}{256}\,, \tag{D3d}$$

$$C_5=-\frac{1}{4}\left(\frac{\Gamma(\frac{19}{8})}{\Gamma(\frac{7}{8})}\right)^2\tan\tfrac{3}{8}\pi\,, \tag{D3e}$$

$$C_6=\frac{1}{4}\left(\frac{\Gamma(\frac{19}{8})}{\Gamma(\frac{7}{8})}\right)^2\tan\tfrac{3}{8}\pi\,[\gamma_E-2\ln 2+\psi(\tfrac{19}{8})-\tfrac{1}{2}\pi\tan\tfrac{15}{8}\pi]\,, \tag{D3f}$$

$$C_7=-(\tfrac{105}{256})^2\,, \tag{D3g}$$

$$C_8=(\tfrac{105}{256})^2[-4\ln 2+2\gamma_E+2\psi(\tfrac{23}{8})-\pi\tan\tfrac{3}{8}\pi-1]\,, \tag{D3h}$$

and

$$C_9=-(\tfrac{105}{256})^2[(1+4\ln 2-2\gamma_E)(-\psi(\tfrac{23}{8})+\tfrac{1}{2}\pi\tan\tfrac{3}{8}\pi)+\psi^2(\tfrac{23}{8})$$

$$-\pi\psi(\tfrac{23}{8})\tan\tfrac{3}{8}\pi+\tfrac{1}{2}\psi'(\tfrac{23}{8})-\tfrac{1}{4}\pi^2-\gamma_E+2\ln 2-\tfrac{1}{8}]\,, \tag{D3i}$$

where $\Gamma(x)$ is the gamma function and $\psi(x)=d\ln\Gamma(x)/dx$. The numerical values of $C_i$, $i=1, 2, \ldots, 9$, are given in Table I.

We can obtain the large-$y$ behavior of $X_+^{(2n-1)}(y)$ and $X_-^{(2n)}(y)$ from the small-$t$ behavior of $f^{(2n)}(t)$ and $g^{(2n-1)}(t)$ [see (C7) and (C8)]. In Ref. 13 it was shown that

$$f^{(2n)}(t) \sim \sum_{k=1}^{2n} a_{n,k}(\ln t)^k + O(1) \quad \text{as } t \to 0 \tag{D4}$$

and

$$g^{(2n-1)}(t) \sim \sum_{k=1}^{2n-1} b_{n,k}(\ln t)^k + O(1) \quad \text{as } t \to 0 \, . \tag{D5}$$

If we now use (D4), (D5), (C12), and (C14) in (C17) and (C18), then (2.8) and (2.9) follow. From (D4) and (D5) one might expect the leading large-$y$ behavior of $X_+^{(2n-1)}(y)$ $[X_-^{(2n)}(y)]$ to be $(\ln y)^{2n-1}/y^2$ $[(\ln y)^{2n}/y^2]$ instead of (2.8) [(2.9)], but a simple computation shows that the coefficient coming from the Fourier transform that multiplies $(\ln y)^{2n-1}y^{-2}$ $[(\ln y)^{2n}y^{-2}]$ vanishes. We have already seen a special case of this in $X_+^{(1)}(y)$ and $X_-^{(2)}(y)$ [for example, $\hat{F}_-^{(2)}(t) \sim (\ln t)^2$ as $t \to 0$ but $X_-^{(2)}(y) \sim (\ln y)/y^2$ as $y \to \infty$].

## APPENDIX E: SMALL-$y$ PROPERTIES OF $X_\pm(y)$

We write $X_+(y)$ as

$$X_+(y) = 2^{5/4}(\sinh 2\beta_c E_1 + \sinh 2\beta_c E_2)^{1/8}(1+y^2)^{-1} + R(y) \, , \tag{E1}$$

where

$$R(y) = \sum_{n=2}^{\infty} X_+^{(2n-1)}(y) \tag{E2}$$

and $X_+^{(2n-1)}(y)$ is defined by (2.1)–(2.3). We expand $R(y)$ as

$$R(y) = \sum_{j=0}^{\infty} (-1)^j R_{2j}^{>} y^{2j} \tag{E3}$$

$$= \sum_{n=2}^{\infty} \sum_{j=0}^{\infty} (-1)^j R_{2j}^{(2n-1)} y^{2j} \tag{E4}$$

or

$$R_{2j}^{>} = \sum_{n=2}^{\infty} R_{2j}^{(2n-1)} \, , \tag{E5}$$

where $R_{2j}^{(2n-1)}$ is the contribution to $R_{2j}^{>}$ coming from the $(2n-1)$th particle cut. From (C38) we easily see that

$$R_{2j}^{(2n-1)} = \frac{(2j+1)!!}{2^j j!} \overline{R}_{2j}^{(2n-1)} \, , \tag{E6}$$

where

$$\overline{R}_{2j}^{(2n-1)} = 2\pi 2^{1/4}(\sinh 2\beta_c E_1 + \sinh 2\beta_c E_2)^{1/8} \int_1^\infty dy_1 \cdots \int_1^\infty dy_{2n}(y_1 + \cdots + y_{2n})^{-2j-2} \mathcal{F}_+^{(2n-1)}(y_1, \ldots, y_{2n}) \, . \tag{E7}$$

We can numerically evaluate (E7) by multiple Gaussian integration methods for $n=1$ and $n=2$. In Table X we give for the symmetrical lattice $\overline{R}_{2j}^{(3)}$ and $\overline{R}_{2j}^{(5)}$ for $j=1$, 2, 3, 4, and 5. We now approximate $R_{2j}^{>}$ by

$$R_{2j}^{>} \simeq R_{2j}^{(3)} + R_{2j}^{(5)} \, , \tag{E8}$$

which gives $R_{2j}^{>}$ to (at least) six decimal places (see Table III). Higher accuracy can be obtained by improving our estimates for $R_{2j}^{(3)}$ and $R_{2j}^{(5)}$ and considering the contribution from the higher-order terms, i.e., $R_{2j}^{(7)}$, $R_{2j}^{(9)}$, etc. We should note that (B7) is (from a numerical point of view) ill-suited to compute the coefficients $R_{2j}^{>}$ since in (B7) the pole term is not explicitly separated from the $R(y)$ term. Given the coefficients $R_{2j}^{>}$ we can compute the coefficients $\Sigma_{2j}^{+}$ of (2.14). Straightforward algebra shows that

$$\begin{aligned}
\Sigma_2^+ &= 1 - \beta_2 \, , \\
-\Sigma_4^+ &= -\beta_2 + \beta_2^2 - \beta_4 \, , \\
\Sigma_6^+ &= \beta_2^2 - \beta_4 - \beta_6 + 2\beta_2\beta_4 - \beta_2^3 \, , \\
-\Sigma_8^+ &= -\beta_6 + 2\beta_2\beta_4 - \beta_2^3 - \beta_8 + \beta_4^2 + 2\beta_2\beta_6 - 3\beta_2^2\beta_4 + \beta_2^4 \, ,
\end{aligned} \tag{E9}$$

and

$$\Sigma_{10}^+ = -\beta_8 + \beta_4^2 + 2\beta_2\beta_6 - 3\beta_2^2\beta_4 + \beta_2^4 - \beta_{10} + 2\beta_2\beta_8 + 2\beta_4\beta_6 - 3\beta_2\beta_4^2 - 3\beta_2^2\beta_6 + 4\beta_2^3\beta_4 - \beta_2^5 \, ,$$

where

$$\beta_{2j} = (-1)^j(R_{2j}^{>} - R_{2j-2}^{>})/X_+(0) \, . \tag{E10}$$

To obtain the small-$y$ properties of $X_-(y)$ we write

$$X_-(y) = \sum_{j=0}^{\infty} R_{2j}^{<}(-1)^j y^{2j} \tag{E11}$$

and

TABLE X. Coefficients $\overline{R}_{2j}^{(3)}$ and $\overline{R}_{2j}^{(5)}$ for $j=1,2,\ldots,5$. See Eqs. (E5) and (E6).

| $j$ | $\overline{R}_{2j}^{(3)}$ | $\overline{R}_{2j}^{(5)}$ |
|---|---|---|
| 1 | $0.189\,202\,162\times10^{-4}$ | $0.39\times10^{-9}$ |
| 2 | $0.444\,089\,652\times10^{-6}$ | $0.5\times10^{-12}$ |
| 3 | $0.158\,202\,249\times10^{-7}$ | $0.1\times10^{-14}$ |
| 4 | $0.714\,385\,994\times10^{-9}$ | $0.6\times10^{-17}$ |
| 5 | $0.376\,279\,852\times10^{-10}$ | $0.4\times10^{-19}$ |

TABLE XI. Coefficients $R_{2j}^{(2)}$ and $R_{2j}^{(4)}$ for $j=1,2,3$, and 4.

| $j$ | $R_{2j}^{(2)}$ | $R_{2j}^{(4)}$ |
|---|---|---|
| 1 | $0.687\,994\,7517\times10^{-2}$ | $0.1265\times10^{-6}$ |
| 2 | $0.982\,849\,645\times10^{-3}$ | $0.8360\times10^{-9}$ |
| 3 | $0.163\,808\,2742\times10^{-3}$ | $0.9715\times10^{-11}$ |
| 4 | $0.297\,833\,2258\times10^{-4}$ | $0.1568\times10^{-12}$ |

$$R_{2j}^{<} = \sum_{n=1}^{\infty} R_{2j}^{(2n)} , \tag{E12}$$

where $R_{2j}^{(2n)}$ is the contribution to $R_{2j}^{<}$ coming from the $2n$th branch cut. From (2.2), (2.3), and (2.5) we have

$$R_{2j}^{(2)} = \int_0^{\infty} \frac{\rho_-^{(2)}(y)}{y^{2+2j}} dy \tag{E13a}$$

$$= \frac{2^{5/4}}{\pi} (\sinh 2\beta_c E_1 + \sinh 2\beta_c E_2)^{1/8} \int_2^{\infty} \frac{(y^2-4)^{1/2}}{y^{4+2j}} dy \tag{E13b}$$

$$= \frac{2^{1/4}}{2^{2j+3}\pi^{1/2}} (\sinh 2\beta_c E_1 + \sinh 2\beta_c E_2)^{1/8} \frac{\Gamma(j+1)}{\Gamma(j+\frac{5}{2})} . \tag{E13c}$$

Thus from (E13c) we can write for $y \to 0$

$$X_-^{(2)}(y) = (2^{1/4}/6\pi)(\sinh 2\beta_c E_1 + \sinh 2\beta_c E_2)^{1/8} \times (1 - \tfrac{1}{10}y^2 + \tfrac{1}{70}y^4 - \tfrac{1}{420}y^6 + \cdots) . \tag{E14}$$

The contribution $R_{2j}^{(4)}$ is

$$R_{2j}^{(4)} = \frac{(2j+1)!!}{2^j j!} \bar{R}_{2j}^{(4)} , \tag{E15}$$

where

$$\bar{R}_{2j}^{(4)} = 2\pi 2^{1/4} (\sinh 2\beta_c E_1 + \sinh 2\beta_c E_2)^{1/8} \int_1^{\infty} dy_1 \cdots \int_1^{\infty} dy_4 \mathfrak{F}_-^{(4)}(y_1, y_2, y_3, y_4)(y_1+y_2+y_3+y_4)^{-2j-2} \tag{E16}$$

and $\mathfrak{F}_-^{(4)}$ is given by (C37b). We have numerically evaluated (E16), and through (E15) the quantities $R_{2j}^{(4)}$ for $j = 1, 2, 3$, and 4. The results (for the symmetric lattice) are given in Table XI.

We now make the approximation

$$R_{2j}^{<} \simeq R_{2j}^{(2)} + R_{2j}^{(4)} , \tag{E17}$$

which is accurate to six to seven places. Given the coefficients $R_{2j}^{<}$ we can easily compute $\Sigma_{2j}^{-}$ of (2.14). The coefficients $R_{2j}^{<}$ are in Table III and $\Sigma_{2j}^{-}$ in Table IV.

*Supported in part by Grant No. DID71-04010-A02 of the National Science Foundation.
†Supported in part by Grant No. H037758 of the National Science Foundation.
‡Alfred P. Sloan Fellow.

[1]L. P. Kadanoff, Physics 2, 263 (1966); L. P. Kadanoff, W. Götze, D. Hamblen, R. Hecht, E. A. S. Lewis, V. V. Palciauskas, M. Rayl, J. Swift, D. Aspnes, and J. Kane, Rev. Mod. Phys. 39, 395 (1967).
[2]M. E. Fisher, J. Math. Phys. 5, 944 (1964).
[3]M. E. Fisher, Rep. Prog. Phys. 30, 615 (1967).
[4]L. S. Ornstein and F. Zernike, Proc. Acad. Sci. Amsterdam 17, 793 (1914); Z. Phys. 19, 134 (1918); 27, 761 (1926).
[5]M. E. Fisher and R. J. Burford, Phys. Rev. 156, 583 (1967).
[6]D. S. Ritchie and M. E. Fisher, Phys. Rev. B 5, 2668 (1972).
[7]M. E. Fisher and A. Aharony, Phys. Rev. Lett. 31, 1238 (1973); Phys. Rev. B 10, 2818 (1974).
[8]H. B. Tarko and M. E. Fisher, Phys. Rev. Lett. 31, 926 (1973); Phys. Rev. B 11, 1217 (1975).
[9]M. Ferer, M. A. Moore, and M. Wortis, Phys. Rev. Lett. 22, 1382 (1969).
[10]M. Ferer and M. Wortis, Phys. Rev. B 6, 3426 (1972).
[11]E. Barouch, B. M. McCoy, and T. T. Wu, Phys. Rev. Lett. 31, 1409 (1973).
[12]C. A. Tracy and B. M. McCoy, Phys. Rev. Lett. 31, 1500 (1973). For a discussion concerning the maximum of the $k$-dependent susceptibility for fixed $k$ and $T > T_c$ see C. A. Tracy and B. M. McCoy, Phys. Lett. A 46, 371 (1974). Equation (3) of the second reference should read: $y_{OZ}^{*} = (2\nu/\gamma - 1)^{-1/2}$; the eighth line from the top of the second column on p. 372 should read: Using (2) we see ($x_0 = 2^{11/8}$ for the two-dimensional Ising model) that $X_{OZ}(y^*) \approx 0.311\,2740$ and from (7) it follows $X_{FL}(y^*) \approx 0.326\,649$, which are to be compared with the exact value $X_+(y^*) = 0.313\,2168\ldots$.
[13]T. T. Wu, B. M. McCoy, C. A. Tracy, and E. Barouch, Phys. Rev. B (to be published).
[14]J. C. Norvell, W. P. Wolf, L. M. Corliss, J. M. Hastings, and R. Nathans, Phys. Rev. 186, 567 (1969).
[15]M. P. Schulhof, P. Heller, R. Nathans, and A. Linz, Phys. Rev. B 1, 2304 (1970).
[16]A. Tucciarone, H. Y. Lau, L. M. Corliss, A. Delapalme, and J. M. Hastings, Phys. Rev. B 4, 3206 (1971).
[17]R. J. Birgeneau, J. Skalyo, Jr., and G. Shirane, Phys. Rev. B 3, 1736 (1971).
[18]J. H. Lunacek and D. S. Cannel, Phys. Rev. Lett. 27, 841 (1971).
[19]V. P. Warkulwiz, B. Mozer, and M. S. Green, Phys. Rev. Lett. 32, 1410 (1974).
[20]H. Ikeda and K. Hirakawa, Solid State Commun. 14, 529 (1974).
[21]J. Akimitsu and Y. Ishikawa, Solid State Commun. 15, 1123 (1974).
[22]J. S. Lin and P. W. Schmidt, Phys. Rev. A 10, 2290 (1974).
[23]O. W. Dietrich and J. Als-Nielsen, Phys. Rev. 153, 711 (1967).
[24]J. S. Lin and P. W. Schmidt, Phys. Rev. Lett. 33, 1265 (1974).
[25]M. E. Fisher and J. S. Langer, Phys. Rev. Lett. 20, 665 (1968).
[26]Some of these results have previously been given in Ref. 12.
[27]T. T. Wu, Phys. Rev. 149, 380 (1966).
[28]H. Cheng and T. T. Wu, Phys. Rev. 164, 719 (1967).
[29]L. P. Kadanoff, Nuovo Cimento 45, 276 (1966).

[30]See also B. M. McCoy and T. T. Wu, *The Two-Dimensional Ising Model* (Harvard U.P., Cambridge, Mass., 1973).
[31]See also Ref. 13.
[32]A. Z. Patashinskii and V. L. Pokrovskii, Zh. Eksp. Teor. Fiz. 46, 994 (1964) [Sov. Phys.-JETP 19, 677 (1964)]; A. M. Polyakov, Zh. Eksp. Teor. Fiz. 55, 1026 (1968); 57, 271 (1969) [Sov. Phys.-JETP 28, 533 (1969); 30, 151 (1970)]; A. A. Migdal, Zh. Eksp. Teor. Fiz. 59, 1015 (1970) [Sov. Phys.-JETP 32, 552 (1971)].
[33]B. Simon and R. B. Griffiths, Commun. Math. Phys. 33, 145 (1973).
[34]J. Glimm and A. Jaffe, Ann. Inst. Henri Poincaré 21, 27 (1974), also unpublished reports.
[35]G. A. Baker, Jr., J. Math. Phys. 16, 1324 (1975); see also the review article by K. G. Wilson and J. Kogut [Phys. Rep. C 12, 75 (1974)].
[36]J. Hubbard, Phys. Lett. A 39, 365 (1972).
[37]M. E. Fisher, Physica 25, 521 (1959). See also Ref.
[38]G. V. Ryazanov, Zh. Eksp. Teor. Fiz. 49, 1134 (1965) [Sov. Phys.-JETP 22, 789 (1966)].
[39]V. G. Vaks, A. I. Larkin, and Yu. N. Ovchinnikov, Zh. Eksp. Teor. Fiz. 49, 1180 (1965) [Sov. Phys.-JETP 22, 820 (1966)].
[40]M. E. Fisher in *Critical Phenomena*, edited by M. S. Green and J. V. Sengers, Natl. Bur. Stand. (U.S.) Misc. Publ. No. 273 (U. S. GPO, Washington, D.C., 1966), p. 108.
[41]G. Stell, Phys. Lett. A 27, 550 (1968).
[42]R. Hocken and G. Stell, Phys. Rev. A 8, 887 (1973).
[43]K. G. Wilson and M. E. Fisher, Phys. Rev. Lett. 28, 240 (1972).
[44]E. Brézin, D. J. Amit, and J. Zinn-Justin, Phys. Rev. Lett. 32, 151 (1974); E. Brézin, J. C. le Guillou, and J. Zinn-Justin, Phys. Rev. Lett. 32, 473 (1974).
[45]For a discussion of the importance of resolution corrections see J. Als-Nielsen and O. W. Dietrich, Phys. Rev. 153, 706 (1967), and the discussion in Ref. 16.
[46]See the discussion in Ref. 16.
[47]If one uses series estimates of $\gamma$ and $\nu$ for the three-dimensional Ising model and assumes $(2-\eta)\nu=\gamma$, then one obtains $\eta=0.056$. See Ref. 5.
[48]See, for example, G. N. Watson, *A Treatise on the Theory of Bessel Functions* (Cambridge U.P., Cambridge, England, 1966), Chap. XII, p. 440.
[49]See, for example, A. Erdelyi, *Higher Transcendental Functions* (McGraw-Hill, New York, 1953), Vol. I, Chap. 2.
[50]See, for example, Ref. 48, p. 410, Eq. (1).
[51]To obtain $F(1,2;1;z)$ and $F(2,2;1;z)$ from $F(1,1;1;z)$ use Eq. (2), p. 102, of Ref. 49.
[52]See, for example, *Table of Integrals, Series, and Products*, edited by I. S. Gradshteyn and I. M. Ryzhik (Academic, New York, 1965), Eq. 3.1972.
[53]See, for example, *Handbook of Mathematical Functions*, edited by M. Abramowitz and I. A. Stegun (Dover, New York, 1965), Chap. 15, Eq. 15.1.7.
[54]Use Ref. 53 and Eqs. (21) and (24), p. 102 of Ref. 49.